



UNIVERSIDADE ESTADUAL DE CAMPINAS  
Faculdade de Engenharia Elétrica e de Computação

Dandara Thamilys Guedes de Andrade

**Development and Evaluation of Human-Machine  
Interfaces for the Control and Actuation of  
Upper-Limb Prostheses.  
Desenvolvimento e Avaliação de Interfaces  
Homem-Máquina para o Controle e Atuação de  
Próteses de Membros Superiores.**

Campinas

2018



UNIVERSIDADE ESTADUAL DE CAMPINAS  
Faculdade de Engenharia Elétrica e de Computação

Dandara Thamilys Guedes de Andrade

**Development and Evaluation of Human-Machine Interfaces  
for the Control and Actuation of Upper-Limb Prostheses.  
Desenvolvimento e Avaliação de Interfaces  
Homem-Máquina para o Controle e Atuação de Próteses  
de Membros Superiores.**

A Dissertation presented to the School of Electrical and Computer Engineering of the University of Campinas in partial fulfillment of the requirements for the degree of Master of Science in Electrical Engineering, in the field of Computer Engineering.

Dissertação apresentada à Faculdade de Engenharia Elétrica e de Computação da Universidade Estadual de Campinas como parte dos requisitos exigidos para a obtenção do título de Mestre em Engenharia Elétrica, na Área de Engenharia de Computação.

Supervisor: Prof. Dr. Eric Rohmer

Este exemplar corresponde à versão final da tese defendida pelo aluno Dandara Thamilys Guedes de Andrade, e orientada pelo Prof. Dr. Eric Rohmer.

---

Campinas

2018

**Agência(s) de fomento e nº(s) de processo(s):** Não se aplica.

Ficha catalográfica  
Universidade Estadual de Campinas  
Biblioteca da Área de Engenharia e Arquitetura  
Luciana Pietrosanto Milla - CRB 8/8129

An24d Guedes de Andrade, Dandara Thamyls, 1992-  
Development and evaluation of human-machine interfaces for the control and actuation of upper-limb prostheses / Dandara Thamyls Guedes de Andrade. – Campinas, SP : [s.n.], 2018.

Orientador: Eric Rohmer.  
Dissertação (mestrado) – Universidade Estadual de Campinas, Faculdade de Engenharia Elétrica e de Computação.

1. Prótese. 2. Eletromiografia. 3. Carga de trabalho. 4. Interface. 5. Equipamentos de autoajuda. I. Rohmer, Eric, 1974-. II. Universidade Estadual de Campinas. Faculdade de Engenharia Elétrica e de Computação. III. Título.

Informações para Biblioteca Digital

**Título em outro idioma:** Desenvolvimento e avaliação de interfaces homem-máquina para o controle e atuação de próteses de membros superiores

**Palavras-chave em inglês:**

Prosthesis

Electromyography

Work load

Interface

Self-help equipment

**Área de concentração:** Engenharia de Computação

**Titulação:** Mestra em Engenharia Elétrica

**Banca examinadora:**

Eric Rohmer [Orientador]

José Mario de Martino

Eric Fujiwara

**Data de defesa:** 21-03-2018

**Programa de Pós-Graduação:** Engenharia Elétrica

## COMISSÃO JULGADORA - DISSERTAÇÃO DE MESTRADO

**Candidato:** Dandara Thamyls Guedes de Andrade RA: 163685

**Data da Defesa:** 21 de Março de 2018

**Título da dissertação:** Development and Evaluation of Human-Machine Interfaces for the Control and Actuation of Upper-Limb Prostheses.

Desenvolvimento e Avaliação de Interfaces Homem-Máquina para o Controle e Atuação de Próteses de Membros Superiores.

Prof. Dr. Eric Rohmer (Presidente, FEEC/UNICAMP)

Prof. Dr. José Mario de Martino (FEEC/UNICAMP)

Prof. Dr. Eric Fujiwara (FEM/UNICAMP)

A ata de defesa, com as respectivas assinaturas dos membros da Comissão Julgadora, encontra-se no processo de vida acadêmica do aluno.



*To my family and friends.*

# Acknowledgements

I owe my deepest gratitude to my supervisor, Prof. Dr. Eric Rohmer, for the intellectual support, ideas, analyses feedback, trust, friendship, and patience. I am very proud of everything I have learned in the past two years under your guidance.

I also want to thank my friends from LCA for all the moments we shared – the good food, the movies, the conversations about academic life, and the advice. You made this process easier to get through. Special thanks to my colleagues in the research group. Guilherme Pereira and Pedro Affonso, who started lost as I were in that first Fuzzy Logic class. Antonio Ribas for the numerous advice and of course for reviewing my papers including this one. Amadeu Junior, for all the support inside the laboratory and outside helping me to find the best house I could have hoped to live in Campinas. Also, to Ricardo Taoni who helped me during the data collection phase, without whom I would not have access to the amputee volunteer of this dissertation.

I have had the support, love, and encouragement of my family – my parents, my brother Vivaldo, my cousin Nicole, aunt Rosileia and uncle Geraldo. I am in debt to my uncle Ananisio and to my grandmother Joana who believed and helped me when I was about to give up.

Thanks to Arthur Gusmão for all the food you cooked in past two years, specially when I was too busy cursing my work, and for being extraordinarily tolerant, supportive, and caring. I can never repay everything you have done for us in the last couple of years.

Finally, I would also like to express my gratitude to Fundo de Apoio ao Ensino, à Pesquisa e Extensão (FAEPEX) for their financial support.

*“If we knew what it was we were doing, it would not be called research, would it?”*  
*(Albert Einstein)*

# Resumo

O objetivo desta dissertação é desenvolver e avaliar interfaces para o controle e atuação de próteses de mão. As interfaces desenvolvidas combinam sinais de eletromiografia (EMG) com identificação de rádiofrequência (Módulo RFID), Unidade de Medida Inercial (Módulo de movimento) ou técnicas de visão computacional (Módulo de visão) para selecionar os tipos de interação. Os sinais EMG são responsáveis por desencadear o sistema, enquanto os outros sensores são responsáveis pela seleção da preensão para que o usuário possa interagir com o ambiente. As interações do usuário com a prótese podem ser vistas em uma simulação. A avaliação das três interfaces foi realizada utilizando o Nasa Task Load Index, que acessa a carga de trabalho dos usuários ao usar o sistema para executar tarefas. Essa avaliação acessa níveis de Demanda Mental, Demanda Física, Demanda Temporal, Esforço, Desempenho e Frustração para calcular a carga de trabalho geral das tarefas. Os resultados mostram que o Módulo RFID é a interface que requer menos esforço cognitivo do usuário, seguido pelo Módulo Visão e o Módulo de Movimento, respectivamente. Adicionalmente, o fato de os usuários das interfaces não necessitarem realizar várias co-contrações, como acontece nos sistemas mioelétricos, reduz sua carga cognitiva. Uma tabela comparativa das três interfaces enfatiza as vantagens e desvantagens de cada interface em um ambiente instrumentado e não instrumentado.

**Palavras-chaves:** Próteses de Membro Superior; Eletromiografia; Identificação por Radio Frequência; Unidade de Medida Inercial; Visão Computacional; Carga de Trabalho; Esforço Cognitivo.

# Abstract

The purpose of this dissertation is to develop and evaluate interfaces for controlling and actuation of prosthetic hands. The interfaces developed combine Electromyography signals (EMG) with Radio Frequency Identification (RFID Module), Inertial Measurement Unit sensor (Motion Module) or Computer Vision techniques (Vision Module) to select the types of interaction. The EMG signals are responsible for triggering the system while the other sensors are responsible for the selection of the grasp so the user can interact with the environment. The user interactions with a prosthesis can be seen in a simulation of the prosthesis. The evaluation of the three interfaces was conducted using the Nasa Task Load Index, that accesses the workload of the users while using the system to perform tasks. This evaluation access levels of Mental Demand, Physical Demand, Temporal Demand, Effort, Performance, and Frustration to calculate the overall workload of the tasks. As the results show, the RFID Module is the interface that requires less cognitive effort from the user, followed by the Vision Module and Motion Module, respectively. Additionally, the fact that the users of the interfaces do not need to perform various co-contractions as happens on myoelectric systems reduces their cognitive burden. A comparative table of the three interfaces emphasises the advantages and disadvantages of each interface in a controllable and no-controllable environment.

**Keywords:** Upper Limb Prosthesis; Electromyography; Radio Frequency Identification; Inertial Measurement Unit; Computer Vision; Workload; Cognitive Effort.

# List of Figures

Figure 1 – The different types of hand prehension (SCHLESINGER, 1919). . . . .	19
Figure 2 – The different types of hand prehension. (A) Encompass grasp. (B) Lateral grasp. (C) Precision grasp. (LYONS, 1985) . . . . .	20
Figure 3 – The prehensile group of movements. Adapted from Kapandji (2000). . . .	20
Figure 4 – The different types of palmar grips. Adapted from Kapandji (2000). . . .	21
Figure 5 – The different types of grips with the help of gravity. Adapted from Kapandji (2000). . . . .	21
Figure 6 – The different types of active prehensile. Adapted from Kapandji (2000). .	21
Figure 7 – The different types of gesture expression grips. Adapted from Kapandji (2000). . . . .	22
Figure 8 – The group of dynamic grasps available in the simulation. (A) Mouse grip: initial motion. (B) Mouse grip: triggering signal – mouse click. (C) Active index grip: initial motion. (D)Active index grip: triggering signal – using a spray bottle for example. . . . .	28
Figure 9 – The group of static grasps available in the simulation. (A) Precision open grip. (B) Precision close grip. (C) Key grip. (D) Column grip. (E) Abduction grip. (F) Finger point. (G) Hook grip. (H) Open palm grip. (I) Pinch grip. (J) Power grip. (K)Relaxed hand. (L) Tripod grip. . . . .	28
Figure 10 – Simulation of the prosthetic hand on V-REP. . . . .	29
Figure 11 – Myo Armband Structure. Adapted from Thalmic Labs Inc. (2016a). . . .	30
Figure 12 – EMG readings architecture. . . . .	31
Figure 13 – Motion module overview. . . . .	32
Figure 14 – Motion module architecture . . . . .	33
Figure 15 – (A) Roll, Pitch, Yaw angles when using Myo armband. (B) Contraction with the back of the hand up. (C) Contraction with the back of the hand to the side. (D) Contraction with the back of the hand down. Adapted from Slevinsky (2014) . . . . .	34
Figure 16 – Workflow of motion module. . . . .	35
Figure 17 – Workflow of motion module: grasp selection phase. . . . .	36
Figure 18 – Motion interface feedback prototype. . . . .	38
Figure 19 – Motion interface feedback schematic. . . . .	38
Figure 20 – RFID module overview. . . . .	39
Figure 21 – RFID module architecture . . . . .	40

Figure 22 – Finite state machine of the RFID Module. In the <i>idle</i> state, the prosthetic hand is in the relaxed hand position, and in the final state, $S_2$ , the prosthetic hand reaches one of the 14 grasps showed in Figures 8 and 9. . . .	41
Figure 23 – RFID module workflow. . . . .	42
Figure 24 – RFID module communication diagram. . . . .	45
Figure 25 – Vision module overview. . . . .	46
Figure 26 – Vision module architecture. . . . .	46
Figure 27 – Vision module workflow. . . . .	48
Figure 28 – Vision interface feedback prototype. . . . .	50
Figure 29 – Vision interface feedback schematic. . . . .	51
Figure 30 – Vision interface communication diagram. . . . .	52
Figure 31 – CSI-2 and CCI Transmitter and Receiver Interface. . . . .	53
Figure 32 – Communication architecture of the vision module with a smartphone. . .	53
Figure 33 – NASA TLX comparison cards. . . . .	55
Figure 34 – NASA TLX comparison cards detached. . . . .	55
Figure 35 – Example of rating the scales for Nasa Task Load Index evaluation by a healthy subject. The range of the scale varies from 0 (low) to 100 (high). . . . .	61
Figure 36 – Motion module: raw rating. . . . .	62
Figure 37 – RFID module: raw rating. . . . .	64
Figure 38 – Vision module: raw rating. . . . .	66
Figure 39 – Comparison of workload for the RFID, Vision and Motion modules per subject. . . . .	68
Figure 40 – Comparison of workload for the RFID, Vision and Motion modules with subjects who tested all interfaces. . . . .	69
Figure 41 – Motion module: raw rating. . . . .	71
Figure 42 – RFID module: raw rating. . . . .	72
Figure 43 – Vision module: raw rating. . . . .	74
Figure 44 – Overall workload of the modules – amputee. . . . .	75

# List of Tables

Table 1 – Various types of upper limb prosthesis (KUMAR <i>et al.</i> , 2014). . . . .	23
Table 2 – Possible Interactions with the Prosthesis and Daily Usage Examples. . . .	30
Table 3 – Valid contractions for each module developed . . . . .	31
Table 4 – Examples of interaction with the Motion Module. Direction equal to side/up/down means that the direction of the back of the hand is to the side/up/down. . . .	33
Table 5 – List of materials to build motion module . . . . .	37
Table 6 – List of materials to build RFID module. . . . .	43
Table 7 – Main technical specification of MFRC522 (NXP SEMICONDUCTORS, 2016). . . . .	43
Table 8 – Arduino technical specifications. Adapted from Arduino Company (2017). . . .	44
Table 9 – Contraction and command association. . . . .	45
Table 10 – List of materials to build vision module . . . . .	49
Table 11 – Technical hardware specifications for the Raspberry Pi Camera Module. . . .	50
Table 12 – Interactions performed by the volunteers during the tests. . . . .	57
Table 13 – Information of volunteer's – summary. . . . .	59
Table 14 – Non-amputee volunteer's information. . . . .	60
Table 15 – Amputee volunteer's information. . . . .	60
Table 16 – Values of mean and standard deviation (SD) of each scale analysed in Nasa TLX for the Motion module. . . . .	62
Table 17 – Values of mean and standard deviation (SD) of each scale analysed in Nasa TLX for the RFID module. . . . .	65
Table 18 – Values of mean and standard deviation (SD) of each scale analysed in Nasa TLX for the Vision module . . . . .	66
Table 19 – Mean and standard deviation (SD) of the workload for each module . . . .	69
Table 20 – List of advantages and disadvantages of the interfaces proposed in this work. . .	76



# Contents

<b>List of Figures</b>	<b>11</b>
<b>List of Tables</b>	<b>13</b>
<b>1 Introduction</b>	<b>15</b>
1.1 Justification	15
1.2 Objective	16
1.3 Contributions	16
1.4 Organisation of the Study	16
<b>2 Related Work</b>	<b>18</b>
2.1 The human hand	18
2.2 Prosthetic hands	21
2.3 Summary of the chapter	26
<b>3 Methodology</b>	<b>27</b>
3.1 Simulation of the prosthetic hand	27
3.2 Electromyography (EMG) Sensors Readings with the Myo Armband	29
3.3 Motion Module	32
3.3.1 Workflow of Motion Module	34
3.3.2 List of Materials	37
3.3.3 Schematics	37
3.3.4 Communication Architecture	39
3.4 RFID Module	39
3.4.1 Workflow of RFID Module	41
3.4.2 List of Materials	41
3.4.3 Communication Diagram	43
3.5 Vision Module	44
3.5.1 Workflow of Vision Module	47
3.5.2 List of Materials	49
3.5.3 Schematics	49
3.5.4 Communication Architecture	51
3.6 Procedures	54
3.6.1 NASA Task Load Index (NASA-TLX)	54
3.6.2 The Environment of the Test	55
3.7 Summary of the Chapter	57
<b>4 Results and Discussion</b>	<b>59</b>

4.1	Social Profile of Volunteers . . . . .	59
4.2	Healthy Volunteers . . . . .	60
4.2.1	Motion Module Analysis . . . . .	62
4.2.2	RFID Module Analysis . . . . .	64
4.2.3	Vision Module Analysis . . . . .	66
4.2.4	Healthy Subjects Overall Workload of the Modules . . . . .	67
4.3	Amputee Volunteer . . . . .	70
4.3.1	Motion Module Analysis on Amputee . . . . .	70
4.3.2	RFID Module Analysis on Amputee . . . . .	71
4.3.3	Vision Module Analysis on Amputee . . . . .	73
4.3.4	Amputee Overall Workload of the Modules . . . . .	74
4.4	Summary of the chapter . . . . .	75
	<b>Conclusion . . . . .</b>	<b>77</b>
	<b>Bibliography . . . . .</b>	<b>79</b>
	<b>Appendix . . . . .</b>	<b>83</b>
	<b>APPENDIX A Ethical Committe Approval . . . . .</b>	<b>84</b>
	<b>APPENDIX B Identification Form . . . . .</b>	<b>89</b>
	<b>APPENDIX C Questionnaire . . . . .</b>	<b>91</b>
	<b>APPENDIX D Source code . . . . .</b>	<b>92</b>
	<b>Annex . . . . .</b>	<b>93</b>
	<b>ANNEX A NASA Task Load Index: Rating sheet . . . . .</b>	<b>94</b>

# 1 Introduction

## 1.1 Justification

Nowadays, high-end prosthetic hands are offered to amputees as an efficient device to help them in their daily activities. These prostheses provide their users up to 20 types of grasps, smooth movements, and precise interactions (Touch Bionics Inc., 2018). Nevertheless, the cost of these devices makes them inaccessible for the majority of amputees who need them, especially in countries such as Brazil, where access to prosthetic care can be neglected, and healthcare is expensive if people look for private insurance. Additionally, the training required from the user to control high-end multigrasp prostheses is challenging as it consists on mapping one specific muscular contraction to one grasp. This can be frustrating as users have no guarantee the hands will fit their daily needs if they cannot control them.

However, with the rise of the 3D printing technology, many DIY (Do It Yourself) projects came such as toys for children, music boxes, handbags, jet parts and, among all, prosthetic hands. Due to the reduced cost that 3D printed prostheses offer, this alternative became an accessible and affordable substitute for people who cannot afford prosthetic hands. As an example, a 3D printed prosthetic hand developed at the Galileo University in Guatemala costs \$350 (FAJARDO *et al.*, 2017) while commercial prosthesis with the same functions cost more than \$60000 (BUFFONE, 2013). Still, as available 3D printed hands are mostly non-motorised mechanical in structure, the range of movements they can produce is limited to opening and closing the hand (ENABLE, 2015).

Motorised 3D printed prosthetic projects such as Galileo Hand (FAJARDO *et al.*, 2015) focus on the development of a low-cost multigrasp functional prosthesis. To improve the ways of interaction and control of this kind of prosthesis, this work proposes the development and evaluation of hybrid human prosthetic interactions aiming at the simplification of the interface between the user and the device. With hybrid solutions, the complexity of the commands sent to the prosthesis is simplified once it limits the number of input contractions the user must perform to activate a grasp by compensating with other sensors. This increases the experience of the users with the system, and, consequently, the chances they will keep wearing the prosthetic hand after the first year.

## 1.2 Objective

The primary objective of this work is to study ways to select and trigger patterns of hold and gestures such as interactions used in daily life activities, using hybrid human-machine interfaces for the control of upper-limb prostheses. This work aims to simplify the selection of pre-defined interactions in prosthetic hands. The objective is to limit the input contractions to control a prosthesis by compensating with other sensors. Therefore, innovative ways of interacting with the prosthesis will be investigated using a mixture of electromyography sensors(EMG) along with gesture, Radio Frequency Identification (RFID), or computer vision alongside the scientific approach of selecting a set of hold patterns and gestures to accomplish day-to-day tasks. A simulation was developed to test concepts of Human Machine Interface (HMI) and subsequently train users to calibrate and let them judge about the features of the system before the prosthesis is built.

## 1.3 Contributions

This dissertation contributes to the area of computer engineering. Specifically, it details the architecture of the three interfaces developed to control a prosthetic hand device. These interfaces limit the number of input contractions detected by EMG sensors to control the prosthetic hand and compensate it using other sensors such as RFID, IMU, and a camera. Also, this dissertation evaluates these interfaces from the perspective of the users using the NASA Task Load Index to access the cognitive load required from them while using the interfaces, and, it presents a comparative board with the advantages and disadvantages of the interfaces developed.

## 1.4 Organisation of the Study

The presentation of this work is made in 5 chapters.

In chapter 1, the justification for the development of the research and the objectives were presented.

Chapter 2 presents a review of the literature on the taxonomy of the human hand, different types of prosthetic hands and their different types of control.

In chapter 3, the simulation used in this research is presented as well as the methodology used to develop and evaluate the three hybrid interfaces to control the prosthesis simulation.

In chapter 4, the evaluation of the interfaces using the Nasa Task Load Index is showed and discussed followed by the conclusion of this work. Finally, the URL to the source code used in this project can be found in Appendix D.

## 2 Related Work

This chapter presents a review of the taxonomy of the human hand as well as several models of prosthetic hands that will be specified, followed by the description of different ways that these prostheses are controlled in the environment of research or real life.

### 2.1 The human hand

The hands of humans are a very important, complex and resourceful organ (RHEE *et al.*, 2006). Functions such as open and close the hand are tasks of considerable mechanical complexity that require the simultaneous contraction of several individual muscles (STANDING, 2010). The human hands are basically composed of the wrist joints, carpal and metacarpal bones, and the phalanges. Except for the thumb, all other fingers have three phalanges named proximal phalanges, middle phalanges, and distal phalanges (BRITANNICA, 2016).

Tubiana *et al.* (1996) says the human hand is an organ to obtain sensory information and to execute tasks, having in its anatomy these two functions expressed as indispensable in the relationship of people with the social environment, emphasizing the importance and uniqueness of the upper extremity of the human body.

To discover how humans choose the way objects are grasped, several scientists started studying the grasp taxonomy. According to Cutkosky e Howe (1990), "the taxonomy is a method of organizing the range of human grasp types, and the parameters used in this organization reveal some of the factors influencing grasp choice."

Schlesinger (1919) divided the human grasping in cylindrical, fingertips, hook, palmar, spherical, and lateral as showed in Figure 1. Years later, in 1955, Schwarz e Taylor (1955) summarised these same types of grasp. Three types of grasps were defined by McBride (1942): grasping by the hand as a whole, grasping between the thumb and the fingers and grasping by the combined use of the palm and the digits. Followed by Griffiths (1943) who defined the cylinder, ball, ring, pincer, and pliers grip; and Slocum e Pratt (1946) who highlighted grasp, pinch, and hook grip.

Although these classifications were useful to start the discussion on hand functions, they do not consider any methodology to create the taxonomy. In Griffiths (1943), he does not consider the full potential of the hand since the posture of the hand is conditioned essentially by the shape of the object held. However, one can grasp a cylinder using both cylinder and

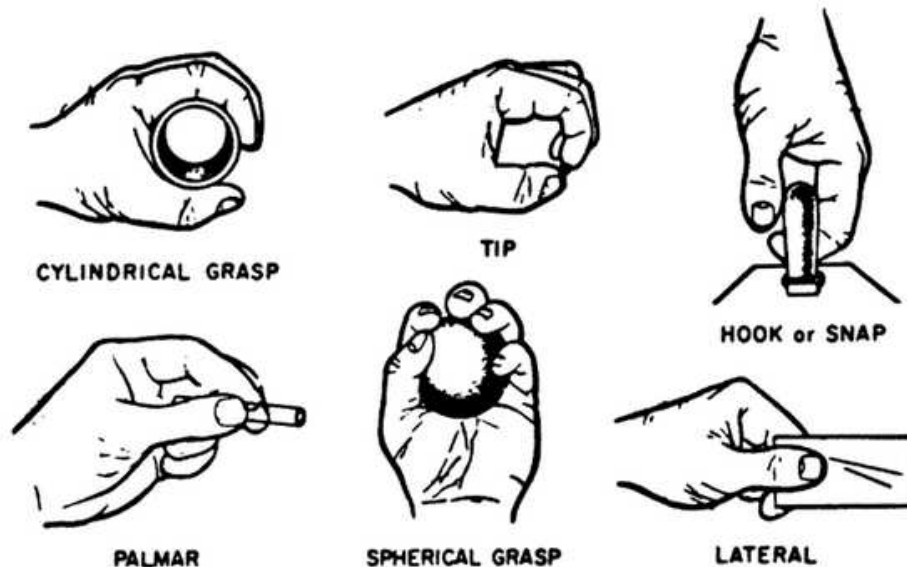


Figure 1 – The different types of hand prehension (SCHLESINGER, 1919).

ball grasp, and both of them will give similar security. It will depend on the purpose of the task one wants to accomplish. Slocum e Pratt (1946) does not analyse the function of the thumb in their taxonomy. While the taxonomy described by McBride (1942) fails to show the anatomical basis for his classification.

Napier (1956) analysed the movements of the hand as a whole and from both the anatomical and functional perspective. He categorised the grasps into power and precision grasp. In precision grip "the object may be pinched between the flexor aspects of the fingers and that of the opposing thumb"; this grasp is related to activities that require sensitivity and dexterity. With the power grip, "the object may be held in a clamp formed by the partly flexed fingers and the palm, counter pressure being applied by the thumb lying more or less in the plane of the palm"; this grasp is related to activities that require stability and security. According to him, these two patterns appear to cover the whole range of prehensile activity of the human hand.

In 1985 the concept of the virtual finger was developed. In sequence, Iberall (1987) describes the types of grasp into three configurations related to the concept of virtual fingers (opposition): the pad for forces between the pads of the fingers and thumb; palm for forces between fingers and the palm; and side for forces between the thumb and the side of index finger. All of these positions are independent and can be used in a single task.

Lyons (1985) defined three types of grasps being the encompass grasp, lateral grasp, and precision grasp. These grasps are showed in Figure 2.

In Cutkosky e Howe (1990), two approaches to study grasp are presented: empirical

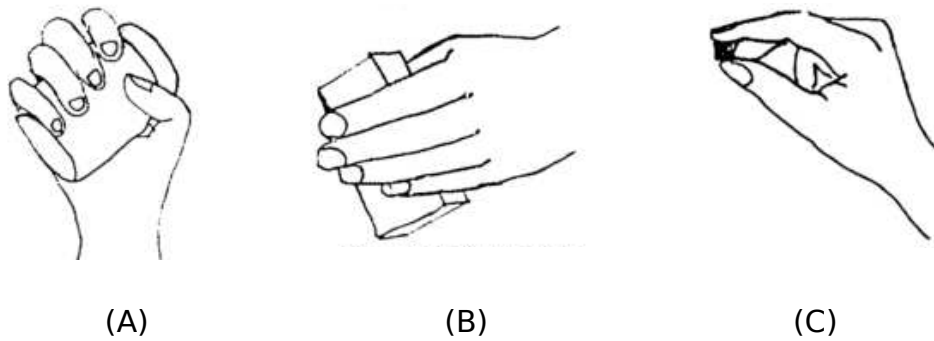


Figure 2 – The different types of hand prehension. (A) Encompass grasp. (B) Lateral grasp. (C) Precision grasp. (LYONS, 1985)



Figure 3 – The prehensile group of movements. Adapted from Kapandji (2000).

and analytical. In the empirical approach, human and animal graspings are the only successful ways known so far. Researchers seem to think that the best way is to learn from the natural systems how to make good artificial ones. However, the variables that humans or animals consider to choose the grasp are not fully known or understood. In the analytical approach, the grasp is modeled from principles: the interaction between the hand and the object and the laws of motion, forces, and physics principles. The problem is that modeling these principles is extremely difficult and much simplification has to be done. Therefore, the model of grasping turns out to work only inside a laboratory, where all the variables involved in the experiment can be controlled.

For Kapandji (2000) the human hand mechanism allows us to have different movements divided into five groups: prehensile, prehensile with the help of gravity, active prehensile or prehensile with action, percussion, and gesture expression.

The prehensile group is the one responsible for precise movements, and it is divided into digital, palmar, and centered. The digital group is subdivided into bidigitals and pluridigitals (see Figure 3). The palmar prehensile are subdivided into palmar-digital, cylindrical-palmar, spherical-palmar, and penta-digital spherical-palmar (see Figure 4).

The grip with the help of gravity makes it possible to grasp objects without the need



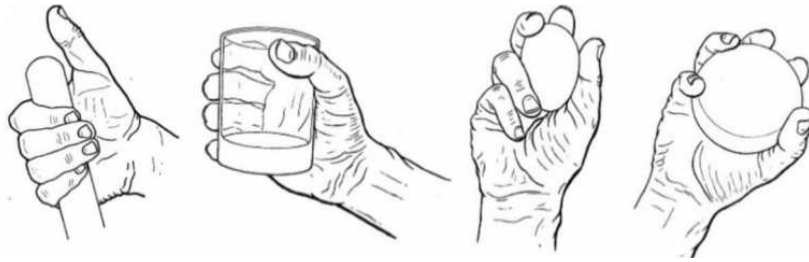


Figure 4 – The different types of palmar grips. Adapted from Kapandji (2000).



Figure 5 – The different types of grips with the help of gravity. Adapted from Kapandji (2000).



Figure 6 – The different types of active prehensile. Adapted from Kapandji (2000).

to use digital tweezers, maintaining the movement less complicated and more structured (see Figure 5). The active prehensile or prehensile with action are responsible for various motion applications, action and reproduction of movements depending on the context and the necessity of the human being in one's daily activity (see Figure 6). In the percussion group, the hand movements are used as an extension of instruments or as instruments of percussion while gesture expressions grips are movements that mean a signal in the social language, such as in Figure 7.

## 2.2 Prosthetic hands

The loss of a limb causes significant effects in the life of people. Besides the notable disability, there is the emotional impact that people go through after the accident and the profound social repercussions after losing the limb, having to be faced as different within the

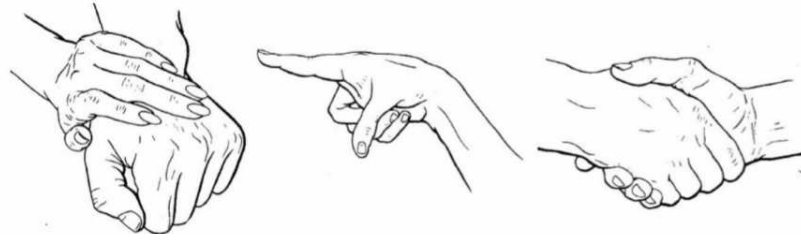


Figure 7 – The different types of gesture expression grips. Adapted from Kapandji (2000).

society they live.

For these reasons, upper limb prostheses have been advancing faster in recent years to improve the quality of life of amputees. According to Kumar *et al.* (2014), the types of prosthetic hands can be separated into two groups: passive and active prosthesis. The passive prostheses also called passive functional prosthetic devices or cosmetic prostheses, are the ones that do not have any movements and are usually used by amputees for cosmetic purposes. Although these prostheses' primary goal is aesthetic, they have some functional features such as pushing, balancing and supporting. The active prosthetic hands have mechanical or electronic parts built in it. Because of this characteristic, the active prosthetic hands tend to be heavier than the passive ones. Active prosthetic hands can also be divided into two types: body powered and externally powered prosthesis.

Body powered prostheses are devices that control the hand of the prosthesis through the movements of the residual limb of the amputee or other parts of the upper body muscles such as shoulders. Externally powered prostheses control the movements of the fingers using motors and are powered by batteries (Ottobock US, 201-) (Orthoworx Orthotics and Prosthetics, 201-). Table 1 presents several types of upper limb prosthetic hands (body powered and externally powered) that can be used by amputees depending on their clinical status.

In the past years, much effort has been made to reduce the cognitive load required by amputees to control externally powered prosthetic upper limbs. These control strategies can be non-hybrid or hybrid. Non-hybrid solutions use only one type of acquisition to control the prosthesis. Hybrid solutions use a combination of input sensors to the control of prosthetic hands.

Some of these control strategies use myoelectric devices (generally using Surface Electromyography or sEMG) and Mechanomyography (MMG) that detects muscular activity when a person contracts the muscles. They can also use Radio-Frequency Identification (RFID) that employs tags to define a specific interaction. Also, Brain-Computer Interface (BCI) can select hand movements by reading brain activity. Computer Vision and deep learning based solutions can use a camera to define the type of interaction with the object in the

Table 1 – Various types of upper limb prosthesis (KUMAR *et al.*, 2014).

Type	Advantages	Disadvantages
Cosmetic	Most lightweight, best cosmetics, less harnessing	High cost if custom made, least function, low cost glove stains easily
Body Powered	Moderate cost, moderate lightweight, most durable, highest sensory feedback, variety of prehensors available for various activities	Requires body movement which may be complex, requires uncomfortable harness, unsatisfactory appearance, increased energy expenditure
Battery powered (myoelectric and/or switch controlled)	Moderate or no harnessing, least body movements needed to operate, moderate cosmetics, more function-proximal areas, stronger grasp in some cases	Heaviest, most expensive, high maintenance, limited sensory feedback, extended therapy time for training
Hybrid (cable to elbow or TD (Terminal Device) and battery powered)	All-cable excursion to elbow or TD	Battery-powered TD weights forearm (harder to lift but good for elbow disarticulation or long THA (Transhumeral Amputation))
If excursion to elbow and battery-powered TD	All-cable excursion to elbow	Lower pinch for TD and least cosmetic
If excursion to TD and battery-powered elbow	Increased TD pinch, all-cable excursion to TD, low effort to position TD, low maintenance	

camera field. Inertial Measurement Unit(IMU) can also be used to define the orientation of movements and activate a hand grasp, and, finally, voice recognition that use spoken words as input to activate the prosthetic hand.

In Barnes *et al.* (2016), an experiment was developed to quantify how "humans can learn to activate upper limb muscles in novel groups and to use these new groups to control a novel myoelectric-controlled interface." The main difference of this approach to other ones that use sEMG to activate prosthetic hands is that Barnes *et al.* (2016) does not use pattern recognition, avoiding issues associated with this kind of methods such as transient changes in EMG (MSC; PHD, 2011). Instead, in this work, they directly link muscle activity to visual feedback and leverage the adaptative behaviour of the user.

To control an Otto Bock prosthetic hand, Murguialday *et al.* (2007) developed an electroencephalogram (EEG)-based motor imagery BCI. This system also includes visual feedback coming from a laptop screen or vibrotactile feedback, both of which proportional to the force the user applied to the object upon grasping. The authors compared the method

using BCI to the method using EMG for controlling a prosthetic hand. Murguialday *et al.* (2007) stated that using the BCI approach "subjects demonstrated the ability to control the prosthetic's grasping force with accuracy comparable to an EMG-based control scheme." However, they claim that attention must be drawn to the fact that the type of feedback used might interfere negatively with the task performance since BCI requires concentration from the user to maintain the Motor Imagery (MI) related to the assignment. Also, in their experiments, the prosthesis did not get to start the movement from the beginning; meaning that during the second stage of the trials, when grasping objects were being tested, the prosthesis was already holding something.

Guo *et al.* (2017) presents a hybrid sensor system for prosthetic manipulation using sEMG combined with mechanomyography (MMG). Their goal is to address the clinical limitations of prostheses control caused by electrode-skin interfaces. MMG is the mechanical signal observable from the surface of a muscle when a person contracts the muscle. Microphones, accelerometers and other devices that can get low-frequency vibration or sound can measure MMG signals. In this paper, the authors investigated two types of non-contact MMG sensors based on accelerometer and microphone. For the experiments, the authors asked nine subjects, two of whom were amputees, to perform some hand movements and then they recorded these movements for 5 seconds. Subjects avoided muscle fatigue during tests resting for several minutes. The results showed that the classification accuracy increases when using combined EMG and MMG features. For the amputee subjects, the classification accuracy increase by 2.7% using aMMG and 4.7% using mMMG.

Trachtenberg *et al.* (2011) introduces a hybrid solution for controlling a prosthetic hand using a myoelectrically operated RFID. The idea of the authors is to send to the prosthesis contextual information when reading the RFID tag in the object so that the prosthesis will reshape the grip that is suitable to interact with the object. They customized an i-Limb Prosthetic Hand to evaluate their solution, and they also combined two types of tests for hand function to assess the functionality of the system described. The results show that, overall, their system performs better than the conventional i-Limb system; in half of their tasks, the RFID method worked faster to grasp an object while for the other half, the timing was very close.

In Oppus *et al.* (2016) the goal of the system is to provide greater flexibility and control over a 3D printed prosthetic hand by combining a brain-computer interface with voice recognition. The two modules, EEG and Voice recognition, available must work together at the same time. The brain waves are measured through the MindWave EEG Headset while the voice recognition module is a device compatible with an Arduino that communicates through a serial port interface. The authors modified an open-source prosthetic hand from

the e-NABLE community and were able to test ten hand gestures with the EEG module and five with the voice recognition modules. According to their results, both modules had high success rates. However, for the EEG module, they only tested the system with two people, and the voice recognition module was tested by two trained people and two non-trained ones.

Condori *et al.* (2016) uses BCI and MI to control a prosthetic hand. They compared two classifiers, the MultiLayer Perceptron (MLP) and the Support Vector Machine (SVM), on an Odroid-xu4 and in a Linux Based PC to analyse processing time and accuracy so they could evaluate the possibility of embedding BCI to a portable, low-cost and trustworthy device. The dataset used was the BCI Competition II, motor imagery dataset III, and the prosthesis used was the Inmoov hand. In their experiments, although both classifiers had the same accuracy, they have very different processing time. Also, they do not integrate the data acquisition hardware to the system, and this step can bring even more delay in processing the information. In a way, their result confirms the computer dependency that BCI technology has. Also, this technique is costly, complicated, and have a high computer dependency. This way, it is hard to think of low-cost prosthesis and BCI in the same product.

In Ghazaei *et al.* (2017), to increase the functionality of a commercial prosthetic hand, the authors developed a deep-learning-based artificial vision system. They divided the objects from their database into four groups of grasps: pinch, tripod, palmar wrist neutral, and palmar wrist pronated. These objects were classified manually regarding proper grip pattern, and to generalise unseen objects they used a Convolutional Neural Network (CNN). This system aims to classify the objects regarding general grasp related features instead of object details. Their results showed 73% of the overall accuracy of the grasping task considering an acceptable error. The feedback from the users was positive towards the system, and, according to the authors, "after about an hour of practice, the participant could accomplish 88% of trials successfully". Nevertheless, their computer-based real-time experiments had better results than the experiments with the subjects. They explain this by claiming the user's behaviour influences the results of the tests. Also, Ghazaei *et al.* (2017) could not provide information about whether the classification of grasps would be more satisfactory for seen or unseen objects.

McMullen *et al.* (2014) developed a hybrid system which uses as input eye tracking and computer vision to identify objects, and BCI (using Intracranial EEG - iEEG) to initiate a semi-autonomous reach-grasp-and-drop of the object using a Modular Prosthetic Limb (MPL). Their system has a supervisory control strategy, and this allows the subjects to execute elaborated motor tasks with a prosthetic hand. The authors made both online and offline tests. Their results show that the subjects reached up to 71.4% of success in performing complex motor tasks using supervisory control. In the online demonstration, the subjects

performed differently: subject 1 had 100% success in performing the entire complex task while subject 2 reached 70% success. The authors explain this behaviour because, for the second subject, they attributed more realistic conditions, while the conditions during tests for subject 1 were not realistic.

After reading recent studies regarding the controlling interface between the operator and prosthetic hands, it is important to realise that most of the studies are trying to eliminate the dependency of EMG only based designs since this controlling system can involve challenging interaction, which requires hard practice from the amputee to be able to control the prosthesis. Following this line of work, chapter 3 will describe three techniques developed for the actuation of upper limb prostheses. The first technique uses a combination of signals from an IMU device and an EMG sensor to control the prosthetic hand, the second one is based on the work of Trachtenberg *et al.* (2011), which uses RFID and EMG sensors to activate grasps in the prostheses, and the third technique uses a combination of EMG and computer vision to activate desired grasps in the prosthetic hand.

## 2.3 Summary of the chapter

This chapter presented some of the most important works on taxonomy for the human hands, an overview of different types of prosthetic hands and the control strategies to select grasps in externally powered prosthesis found in the literature using hybrid and non-hybrid techniques with RFID, voice recognition, brain-computer interfaces and other types of technologies.

## 3 Methodology

This chapter describes three hybrid interfaces to control and actuate in a prosthetic hand to achieve the objectives described in section 1.2. These interfaces are different hybrid solutions for the problem of grasping selection outlined in chapter 1. To visualise the interaction of the interfaces with a prosthesis, a kinematically equivalent simulation of the Inmov prosthesis was developed on the V-REP simulator and it is detailed in section 3.1. To select interactions with the prosthetic hand, the Motion Module presented in section 3.3 uses a combination of EMG and IMU sensors. The RFID Module described in section 3.4 uses EMG sensors combined with readings of RFID tags to select interactions in prosthetic hands; finally, the Vision Module presented in section 3.5, combines computer vision techniques to discover which objects the user is about to interact with and EMG sensors to validate the proposed movement. This chapter also explains in section 3.6 the experiment design and the materials used in the procedures.

### 3.1 Simulation of the prosthetic hand

A robot simulator called V-REP, Coppelia Robotics (ROHMER *et al.*, 2013) is used to simulate the behavior of the prosthetic hand and provide visual feedback on the human-machine interaction. The CAD model adopted in the simulation is available on the Inmoov hand project (LANGEVIN, 201-).

The simulation handles fourteen grasps that can be extended at will. These grasps are divided into two groups - dynamic and static grasps. In this work, a grasp is not simple to hold an object, but it is the ability to hold and to interact with objects, people or the environment around the user; hence, grasps and interactions are indistinctly terms in this text.

The dynamic grasps have subsets of motion to complete desired tasks. The first subset is the initial motion of the prosthesis and the required movement for holding the object. The second subset is the sequence of actions necessary to interact with the object or the environment. Figure 8 illustrates the dynamic grasps available in the simulation. The static group of grasps, however, have a different behavior compared to the dynamic ones. Although static grasps do not mean only to hold an object, they do not have more than one movement configuration. It means that the interactions from this class will not have triggering signals. Figure 9 illustrates the static grasps available in the simulation. A list of daily usage example

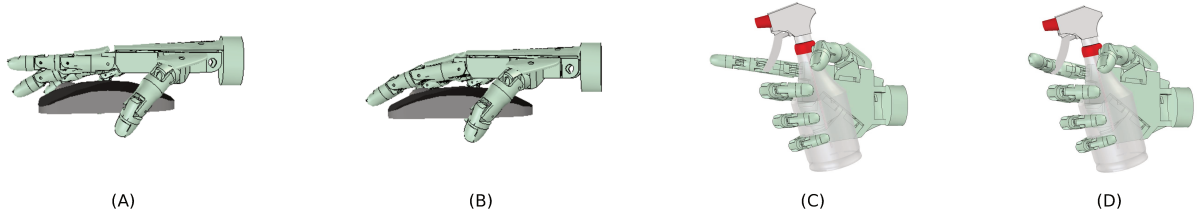


Figure 8 – The group of dynamic grasps available in the simulation. (A) Mouse grip: initial motion. (B) Mouse grip: triggering signal – mouse click. (C) Active index grip: initial motion. (D) Active index grip: triggering signal – using a spray bottle for example.

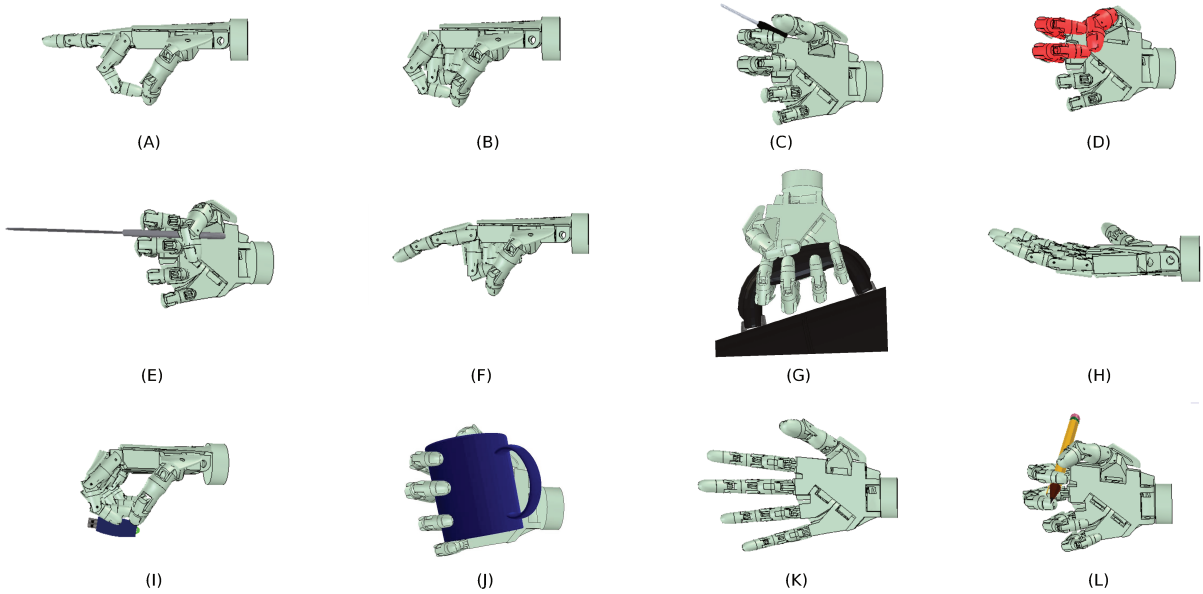


Figure 9 – The group of static grasps available in the simulation. (A) Precision open grip. (B) Precision close grip. (C) Key grip. (D) Column grip. (E) Abduction grip. (F) Finger point. (G) Hook grip. (H) Open palm grip. (I) Pinch grip. (J) Power grip. (K) Relaxed hand. (L) Tripod grip.

for each grasp is showed in Table 2 as well as to where in the taxonomy described by Kapandji (2000) these grasps are included.

Each interaction in the prosthetic hand is defined by a structure that has the time limit to perform actions, a pointer to the next move index, and the position of the slider. A slider is a structure in the simulation that controls the position of each joint of the fingers, and it ranges from 0 (open finger) to 1000 (closed finger). Figure 10 presents the prosthetic hand in the simulator. The orange circle highlights the sliders.

To activate each interaction in the simulation with the interfaces developed, a UDP (User Datagram Protocol) communication-based architecture was used. The simulation (implemented on V-REP) will receive from the controller of the interface the command that will position the hand in the desired grasp. The simulation recognises two types of commands –



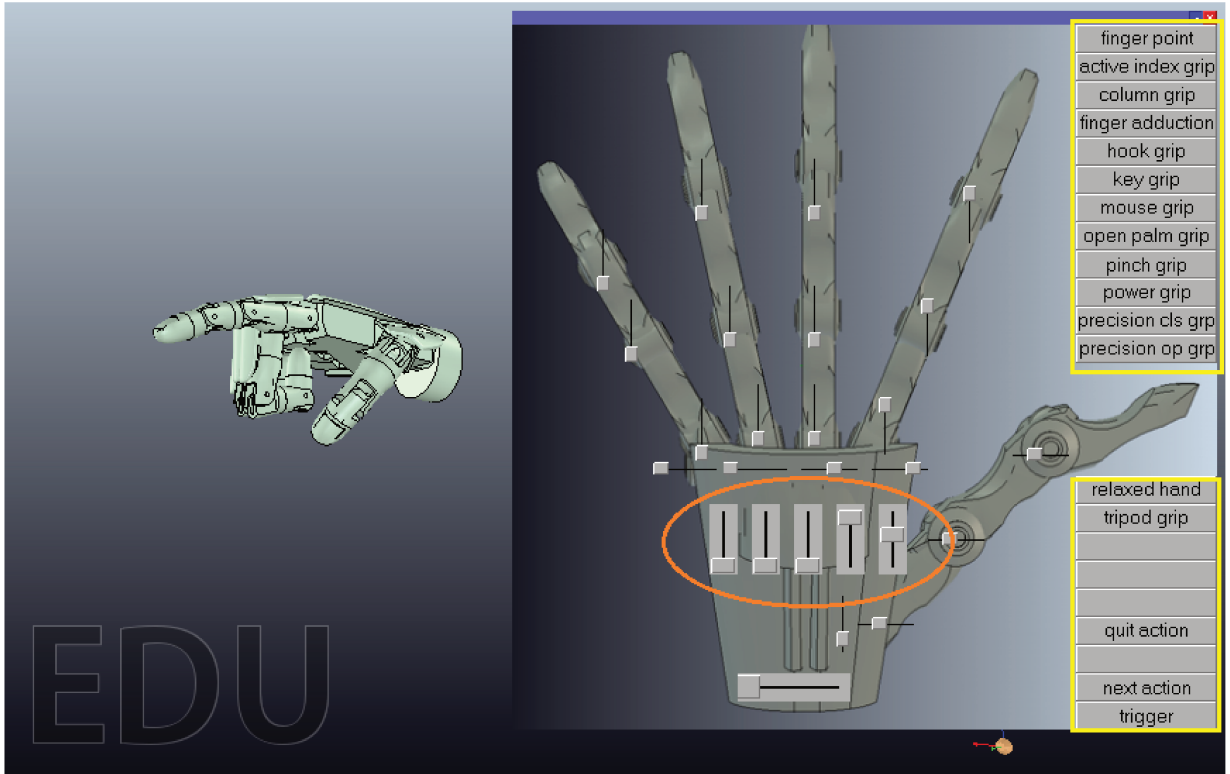


Figure 10 – Simulation of the prosthetic hand on V-REP.

the full name of the interaction or the number of those interactions as listed in Table 2.

It is also possible to send to V-REP the desired interaction through TCP/IP protocol in the format showed in Equation 3.1, where the string sent to the simulator has to be a valid interaction name (yellow box in Figure 10). However, since the UDP protocol is faster to communicate than the TCP/IP protocol, it will be the one used with the modules described later.

$$\backslash*[a-z]+\backslash* \quad (3.1)$$

### 3.2 Electromyography (EMG) Sensors Readings with the Myo Armband

The Myo armband (Thalmic Labs Inc., 2016b) is a standard part of all modules described in this chapter. It is necessary to acquire the EMG signals that are used as one of the inputs to control the hybrid interfaces developed, as well as the IMU signals used in the Motion Module.

Table 2 – Possible Interactions with the Prosthesis and Daily Usage Examples.

Interaction Number	Interaction Name	Example of Use	Taxonomy
0	Relaxed hand	Default hand gesture. Helps to get a natural position	Functional position by (STANDING, 2010)
1	Active index grip	To use with a spray bottle	Active prehensile
2	Column grip	To turn the lights on/off	Percussion
3	Abduction grip	To hold a knife	Bidigital
4	Finger point	To type on a keyboard	Gesture expression or Percussion
5	Hook grip	To hold bags, suitcases	Grip with help of gravity
6	Key grip	To grip spoons	Bidigital
7	Mouse grip	Specifically to hold and click a mouse	Active prehensile
8	Open palm grip	To carry plates	Grip with help of gravity
9	Pinch grip	To hold a flash drive	Bidigital
10	Power grip	To hold a glass of water	Palmar
11	Precision close grip	To play with a magic cube	Bidigital
12	Precision open grip	To manipulate small objects accurately	Bidigital
13	Tripod grip	To manipulate pens	Pluridigital

The structure of the Myo Armband is shown in Figure 11. It is composed by dual indicator LEDs that inform the level of the battery and Bluetooth connection; a nine-axis IMU (three-axis accelerometer, three-axis gyroscope, and three-axis magnetometer), and 8 EMG sensors. Moreover, the armband has an Arm Cortex M4 Processor, a haptic feedback sensor that can create short, medium and long vibrations (Thalmic Labs Inc., 2016b). The Myo armband has a built-in rechargeable lithium-ion battery that can last a full day with one charge. To recharge, one needs only to connect a standard micro-USB cable on the device. Moreover, it is compatible with Windows 7 and higher, Mac OS X 10.8 (Mountain Lion) and above (with included USB Bluetooth adapter), IOS 7.0 and higher, and Android 4.3 and higher, however, the device must have Bluetooth radio that supports Bluetooth 4.0 LE. Although the Myo does not have official support for Linux Operating System, (ZHU, 2014) provides an interface to communicate with the device within Linux platforms.



Figure 11 – Myo Armband Structure. Adapted from Thalmic Labs Inc. (2016a).

The user wears this armband in the residual limb (for amputees) or the forearm (for healthy volunteers). Although each module will not use the same set of movements to control the prosthetic device (see Table 3), the way the system processes the EMG signal is the same for all of them, and it is illustrated by Figure 12. The EMG sensors record the electrical activity produced by the muscles of the users and send it through Bluetooth to the Raspberry Pi 3. The armband has a Bluetooth module in it, and the Raspberry Pi 3 establishes the connection through a dongle connected to one of its USB ports. The Myo armband does not have support from Thalmic Lab to be used with Linux based systems. Therefore, the library developed by Zhu (2014) is being used.

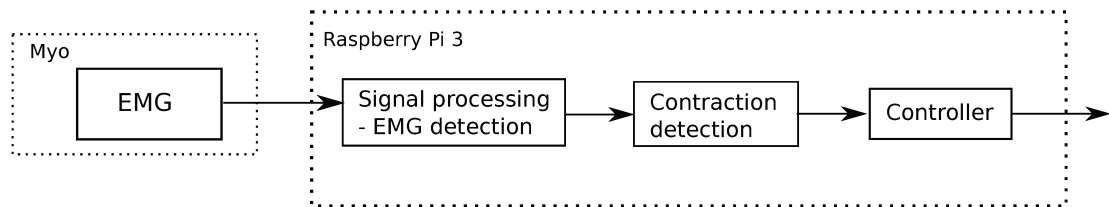


Figure 12 – EMG readings architecture.

When the Raspberry Pi 3 receives the information from the Myo, the stage of signal processing starts. To distinguish the contractions the users make, we are using Myo’s classifier. In this stage, the EMG classifier is enabled as well as a stream of the low-pass filtered EMG signals. The system perceives the EMG signal – rectified and filtered – as a list of  $N$  numbers ( $1 \leq N \leq 8$ ), each one associated with the EMG electrodes presented in the armband. The sampling rate of the underlying EMG sensor is limited to 1 kHz. The frequency at which the EMG signal is taken is 50 Hz, and the cutoff frequency of the low-pass filter is 100 Hz. Then, in the *Contraction detection*, this list of values is processed to sort out valid contractions for each of the modules as in Table 3.

Table 3 – Valid contractions for each module developed

Module	Valid contractions
Motion	Commands Cancel
RFID	Confirm Cancel
Vision	Take picture Confirm or trigger Cancel or next suggestion

### 3.3 Motion Module

The Motion Module is an interface that defines the motion of the fingers in the prosthetic hand based on the combination of EMG signals (contractions), and IMU poses. Therefore, instead of a complex set of EMG signals to decode and map to possible interactions, we reduce the number of signals to map into contraction for command and cancel command, reducing the cognitive load required from the users. Figure 13 shows the overview of the module, where the EMG and IMU sensors are gathered in the Myo armband, the central controller is a Raspberry Pi 3 with Jessie operating system (a Debian release version), and V-REP is the simulator used for visualisation of the interactions with the module.

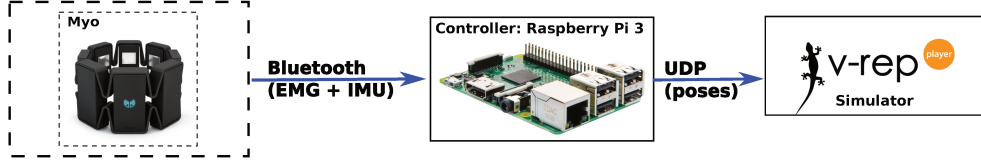


Figure 13 – Motion module overview.

The data from the sensors can be accessed and sent to the controller through Bluetooth. The Controller will process the information received from the Myo and analyse which grasps is associated with the command sent by the user. In this module, a request, or the interaction of the user, is a combination of muscular contractions and the direction pointed out by the IMU device when the user makes this contraction. Table 4 describes the interactions allowed in the module and the respective grasp choice associated with it.

The architecture of the Motion Module is illustrated in Figure 14. The EMG sensors will record the electrical activity produced by the muscles of the users while the IMU device will record the orientation of the arm at the moment of the contraction. When the Raspberry Pi 3 receives the EMG information, as explained in section 3.2, the signal will be processed. This step has a significant effect on the correct behaviour of the module since we discard contractions that users made unwittingly from the ones they intend to be a command.

Parallel to this, a similar process happens to the IMU information. The IMU sensor in the armband sends to the Raspberry Pi 3 the orientation of the arm as a quaternion. The direction of the arm is acquired whenever a user contracts the muscle. In the *Analysis of direction* step on Figure 14, the quaternion is turned into Euler angles through Equation 3.2 and the direction (side, up or down) the user performed the contraction is defined. In this equation,  $\varphi$  is the roll angle, and  $q_0$  to  $q_3$  are real numbers representing the quaternion.

$$\varphi = \arctan \frac{2(q_0q_1 + q_2q_3)}{1 - 2(q_1^2 + q_2^2)} \quad (3.2)$$

Table 4 – Examples of interaction with the Motion Module. Direction equal to side/up/down means that the direction of the back of the hand is to the side/up/down.

Command	Grasp selected
Up (↑) contraction + confirm	Finger point
2x Up (↑) contractions + confirm	Pinch grip
Down (↓) contraction + confirm	Hook grip
2x Down (↓) contraction + confirm	Open palm grip
Side (→ or ←) contraction + confirm	Precision close grip
2x Side (→ or ←) cont. + confirm	Precision open grip
Up (↑) cont. + down (↓) cont. + confirm	Column grip
Up (↑) cont. + side (→ or ←) cont. + confirm	Active index grip
Down (↓) cont. + up (↑) cont. + confirm	Mouse grip
Down (↓) cont. + side (→ or ←) cont. + confirm	Power grip
Side (→ or ←) cont. + up (↑) cont. + confirm	Finger abduction
Up (↑) cont. + 2x down (↓) cont. + confirm	Tripod grip
Up (↑) cont. + 2x side (→ or ←) cont. + confirm	Key grip
Contraction after 3 seconds to any direction	Confirm
Wave out	Cancel
Side (→ or ←) cont. + down (↓) cont. + confirm	Analog (for future implementations)

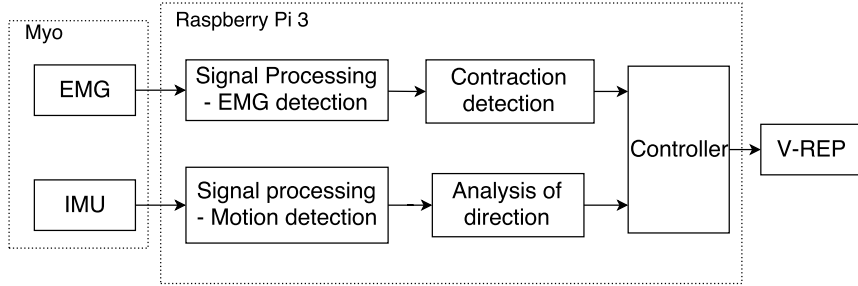


Figure 14 – Motion module architecture

For this step, it is important to highlight that only the  $\varphi$  is taken into account. Since the Myo is placed in the user's forearm as in Figure 15(A), when he turns around his arm to perform contractions,  $\varphi$  is the one that will return the significant information for the movement the user performed. Figures 15(B-D) show the changes the user needs to complete so that the system will receive the pair contraction-detection. Even though the images in this chapter show right-handed examples, the system is designed so that left-handed people can use the armband in their left hand and the behaviour of the module will not change.

Finally, the *Controller* receives the pair contraction-direction, validates this command and associates them to a grasp to send to the simulator through a UDP protocol. Preliminary results of this module can be found in (ANDRADE *et al.*, 2017). The overall flow of control of the system is shown in subsection 3.3.1.

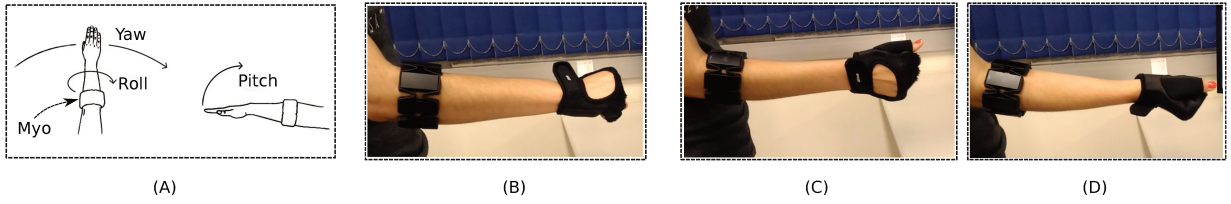


Figure 15 – (A) Roll, Pitch, Yaw angles when using Myo armband. (B) Contraction with the back of the hand up. (C) Contraction with the back of the hand to the side. (D) Contraction with the back of the hand down. Adapted from Slevinsky (2014)

### 3.3.1 Workflow of Motion Module

The motion workflow can be separated into two phases – the calibration phase and the grasp selection phase. The calibration phase is crucial for the correct behaviour of the system since it will calculate the correct range of angles the user has to contract his muscle for the system to work correctly in the grasp selection phase.

As shown in Figure 16, in the calibration phase, the system will ask the user to contract his muscle in specific directions for nine times. This way, three values of angles for each direction is captured and, after this, the minimum, and maximum angle for each direction will be calculated, and those ranges will be the valid ones used in the grasp selection phase to distinguish the direction of the contractions made by the user. Therefore, the grasp selection phase directly depends on the correct calibration of the system. This stage happens every time the user wears the Myo since the position of the IMU changes.

The workflow described in Figure 17 is the grasp selection phase. It depicts how the system works concerning computational and organizational processes. Every time the Myo perceives a contraction in the muscles of the user, the EMG signals go to the system for processing. The highlighted process with dotted lines on Figure 17 is responsible for distinguishing command contractions and involuntary contractions the user performs while holding an object.

When the program perceives a contraction from the user, the system will calculate the average of this signal with Equation 3.3. Then the current average of the signal is compared with the value of the previous contraction. If the current average of the EMG sensors is higher than the last one and if the time passed since the last contraction is greater than 2 seconds, the system considers the current contraction as a strong contraction (there is a command contraction). Otherwise, it is probably an involuntary contraction (weak contraction) made by the user upon manipulating an object. The value of 2 seconds was initially chosen since it reflects the time average needed to differentiate two contractions made on purpose by the

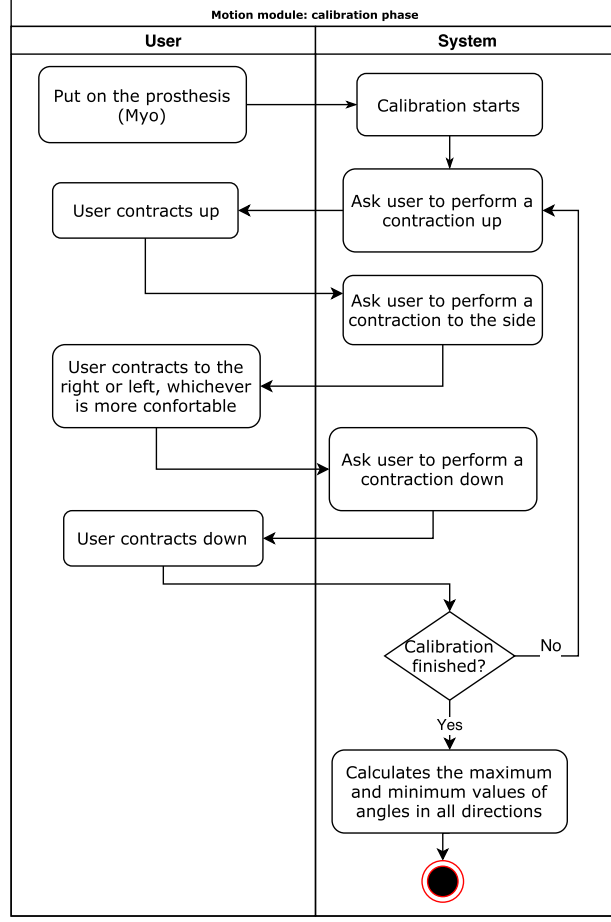


Figure 16 – Workflow of motion module.

user. This time interval is adjustable.

$$\frac{1}{N} \sum_{i=0}^{N-1} EMG[i] \quad (3.3)$$

When the user performs a strong contraction, the system calculates the direction to where the user made this contraction. If the user sends a confirmation contraction, the system will check if that is a valid grasp command and send the position of the fingers to the simulator. Otherwise, it will wait and check the next muscle contraction to be analysed. When the user sends a valid grasp to the simulator, the hand will only change the position of the fingers upon triggers or cancel command. This is necessary to avoid the user dropping the object in the middle of a task that he is supposed to finish.

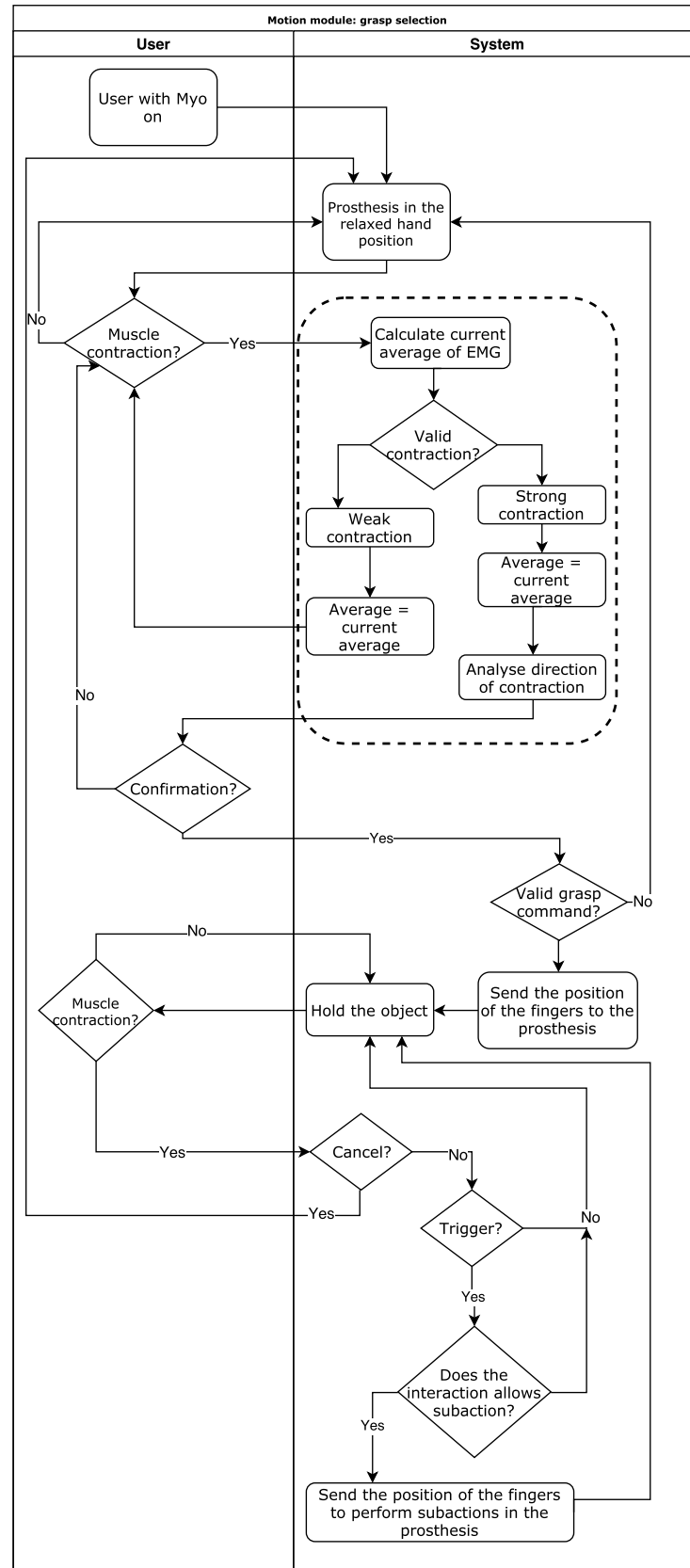


Figure 17 – Workflow of motion module: grasp selection phase.



### 3.3.2 List of Materials

The materials listed on Table 5 were used to build the motion module interface.

Table 5 – List of materials to build motion module

Material	Quantity
Raspberry Pi 3 model B	1
Myo armband	1
Myo bluetooth adapter	1
Yellow LED 5 mm	3
Red LED 5 mm	1
Green LED 5 mm	1
Resistors 1 k $\Omega$	5

### 3.3.3 Schematics

Since to control the prosthesis using the motion interface the users will have to contract their muscles in different orientations, it is essential for the users to become aware if their contractions were made to the right direction. For this, we developed luminous feedback to be coupled in the user's prosthesis. Since a real prosthetic hand was not available for tests, a Printed Circuit Board (PCB), as in Figure 18, was built using KiCad (KiCad EDA, 20–) to illustrate this feedback to the volunteers. This PCB was connected to the system as a shield in the Raspberry Pi 3.

Hence, every time the user contracts his muscles to one direction, one yellow LED is turned on to indicate the direction of the contraction. When the user reaches a valid combination of contraction-direction (Table 4), he can send a confirmation contraction (any contraction made after the green LED turns on, which takes 3 seconds after the last contraction was made). As soon as the user performs the confirmation contraction, the system sends the corresponding interaction to VREP. To return to the initial state (relaxed hand position), the user must perform a cancelation contraction; when this happens, the red LED is turned on to indicate the interaction is over.

The PCB on Figure 18 was built from the schematic in Figure 19. In this schematic, P1 is the Raspberry Pi 3, R1 to R5 are 1 k $\Omega$  resistors, D1 to D3 are the LEDs that represent the direction of the contractions (yellow LEDs), where D1 is "front", D2 is "right" (for right-handed people), and D3 is "down". The D4 is the cancelation LED (red), and D5 is the confirmation LED (green).

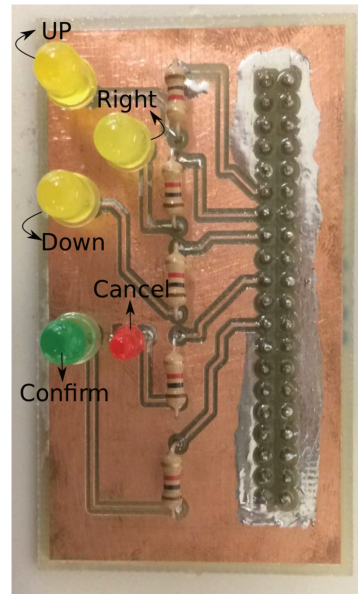


Figure 18 – Motion interface feedback prototype.

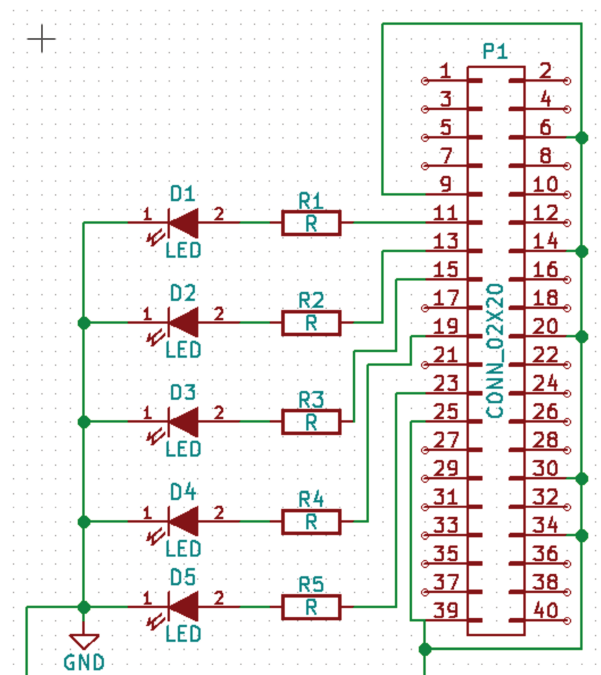


Figure 19 – Motion interface feedback schematic.

### 3.3.4 Communication Architecture

Figure 13 depicts the communication diagram of the motion interface. The EMG and IMU sensors are gathered in the Myo armband, which communicates with the central Controller by Bluetooth. The Controller will process the information received from the Myo and analyse which of the fourteen grasps described in section 3.1 is associated with the command sent by the user. When the data is processed in the controller, it will send through UDP protocol the corresponding interaction to be visualised on V-REP.

Regarding communication architecture, this module is the simplest to be implemented since the controller needs only to communicate with the simulator and the sensors, which are gathered on the same device (Myo armband).

## 3.4 RFID Module

In this module, the motion of the fingers in the prosthetic hand is defined by the RFID tag readings the system performs and by contractions the user does to confirm or to cancel commands. Similarly to the motion module, there is no need to map a complex set of EMG signals into interactions due to its hybrid approach. Instead, the choice of interactions is based on two types of contractions (confirm and cancel commands) and the system uses RFID tags placed on devices (e.g., on a mouse), close to devices (e.g. besides a keyboard), or in the pocket of the user to select the grasping to be triggered.

Figure 20 shows the overview of this module. An RFID reader is coupled to the prosthetic device, and an RFID tag is attached to objects. When the prosthesis approaches the tagged object, the tag is read, and after the confirmation contraction from the user, the corresponding command to interact with this object is sent to the prosthesis.

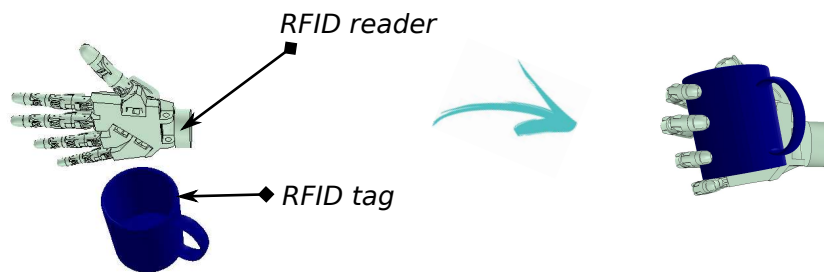


Figure 20 – RFID module overview.

The architecture of the RFID Module is shown on Figure 21. The EMG signals processing happens according to section 3.2 and the contractions from the user are classified into confirmation or trigger contractions and canceling contractions. Regarding the subsys-

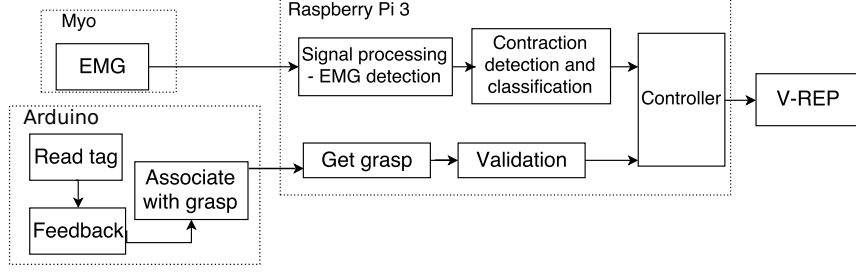


Figure 21 – RFID module architecture

tem role in the system, the first process showed in the architecture is the reading of the RFID tag. When this process finishes, a LED is turned on as visual feedback for the user; this is important to allow him to know that a tag has been read by the system successfully. In sequence, the tag that was read is associated with a preprogrammed grasp in the prosthesis. Then, the Raspberry Pi 3 receives this information and validates it since it is possible for the system to read a tag which does not represent a type of grasp the prosthesis can reach. After validation, the grasp is sent to the *Controller* box, which reads the grip and sends it to V-REP for its actuation.

The state machine on Figure 22 illustrates all the interactions the user can have with the system. As soon as the user wears the prosthesis, it will be in the relaxed hand position (*Idle State*). When the user approaches an object that has an RFID tag on it, the system reads the tag and goes to the state  $S_1$ , where it waits for three commands: read another tag, confirmation or cancel. The confirmation contraction tells the system to go to the state  $S_2$ , where the grasp is performed, and the state machine waits for other commands. Otherwise, the user can perform a cancel contraction, which tells the system that the user wants to cancel the current grasp and go back to state *Idle*. The third command is to read another tag; the user might approach another object, the RFID tag on this object is read, and the system remains on state  $S_1$  (waiting for other commands).

Once the state machine is in state  $S_2$ , the user can perform the cancel command, can approach an object to read the tag on it or can carry out the trigger control. The trigger is only available for dynamic grasps of the set and is also activated by a contraction equal to the confirmation contraction. What differentiates one command from the other is the current state of the machine.

When entering state  $S_3$ , the trigger is sent to the prosthesis, the grip is performed on V-REP, and the state automatically changes back to the state  $S_2$ , so the user can either

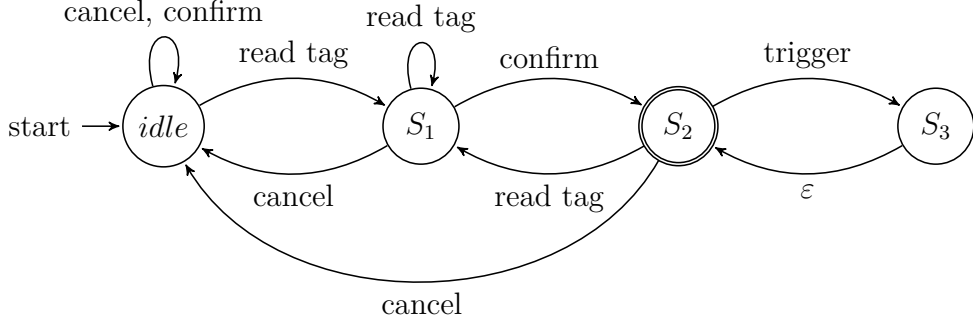


Figure 22 – Finite state machine of the RFID Module. In the *idle* state, the prosthetic hand is in the relaxed hand position, and in the final state,  $S_2$ , the prosthetic hand reaches one of the 14 grasps showed in Figures 8 and 9.

continue sending triggers to the prosthesis or do something else. Preliminary results of this module can also be found in (ANDRADE *et al.*, 2017). The detailed workflow of this module is illustrated on subsection 3.4.1.

### 3.4.1 Workflow of RFID Module

The first thing to observe in the workflow is the active role of the central controller managing not only the inputs of the user but also the inputs from the Arduino in charge of reading the RFID sensor values. Figure 23 shows that the system prevents the prosthetic device to drop the object while the user is finishing a task. The prosthesis only drops the object when the user performs a cancel command. Unlike the Motion Module, the user does not have to remember any combination of contraction to select the desired interaction. The only contractions the user has to learn to control the interface is the cancel and confirm/trigger contractions.

Moreover, one can see that not all interactions allow triggers commands to be sent to the prosthesis, which saves the computational resource. The list of materials to build this module and the specifications are described in subsection 3.4.2.

### 3.4.2 List of Materials

The materials listed on Table 6 were used to build the RFID module interface. The RFID reader used was the MFRC522, and its main characteristics are described in Table 7. An Arduino Uno was used, its main technical specifications are described in Table 8.

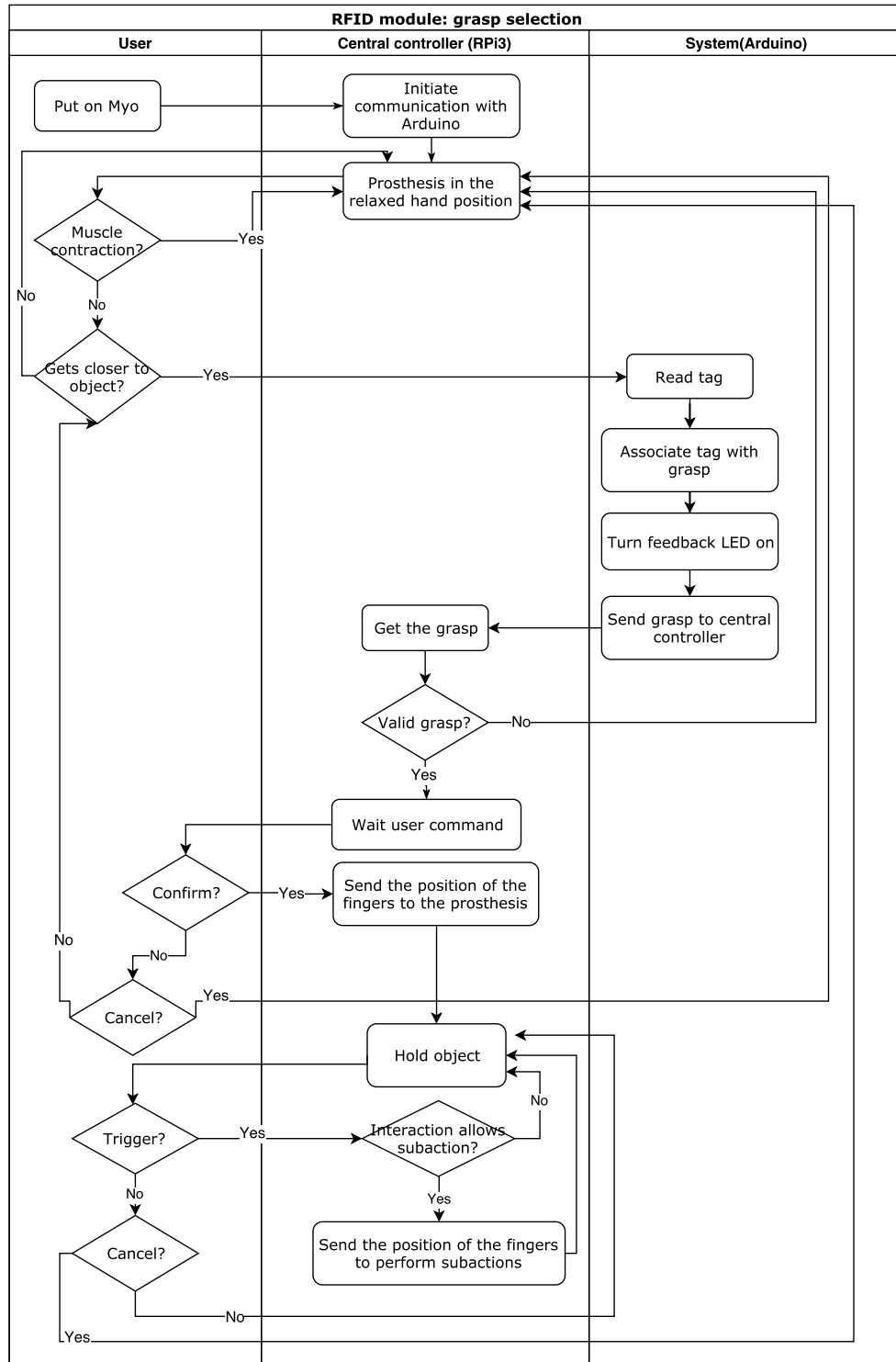


Figure 23 – RFID module workflow.

Table 6 – List of materials to build RFID module.

Material	Quantity
Raspberry Pi 3 model B	1
Myo armband	1
Myo bluetooth adapter	1
RFID reader	1
Arduino uno	1
LED 5 mm or Buzzer	1

Table 7 – Main technical specification of MFRC522 (NXP SEMICONDUCTORS, 2016).

MFRC522	Technical specification
Communication frequency	13.56 MHz
Host interfaces provided	SPI up to 10 Mbit/s RS232 UART up to 1228.8 kBd in Fast mode or up to 3400 kBd in High-speed mode $I^2C$ up to 400 kBd
Typical operating distance	50 mm (depending on the antenna)
FIFO buffer	handles 64 byte send and receive
Power supply	2.5 V to 3.3 V

### 3.4.3 Communication Diagram

Despite using a Myo armband to acquire EMG signals from the user, this module does not get information from the IMU device present on it as in the motion interface. The armband communicates with the central controller (Raspberry Pi 3) through Bluetooth. As seen in Figure 24, another difference between this module and the previous one described is that an Arduino is used as an intermediate device to read the RFID tags. This choice was made because it is possible to replace the RFID based controller with an Android device. Therefore, the intelligence inside the controller can be transferred to a smartphone, while the microcontroller keeps handling the peripherals of the system. Moreover, having an Arduino controlling the lower layers of peripherals is desirable to take the processing overhead from the central controller.

The RFID reader communicates with the Arduino through SPI bus since the MFRC522 library for Arduino only supports the SPI communication interface. The Arduino then communicates with the central controller using the serial bus, through which the Arduino sends

Table 8 – Arduino technical specifications. Adapted from Arduino Company (2017).

Arduino uno	Technical specification
Microcontroller	ATmega328P
Operating Voltage	5 V
Input Voltage (recommended)	7-12 V
Input Voltage (limit)	6-20 V
Digital I/O pin	14
PWM digital I/O pins	6
Analog input pins	6
DC Current per I/O Pin	20 mA
DC Current for 3.3 V Pin	50 mA
Flash memory	32 KB
SRAM	2 KB
EEPROM	1 KB
Clock speed	16 MHz
Length	68.6 mm
Width	53.4 mm
Weight	25 g

the information the Controller needs to suggest a grasp for the user. Finally, the controller sends the poses of the fingers to the simulated hand by using the UDP protocol.

### 3.5 Vision Module

The vision module is also a hybrid approach to simplify the controlling interface of a prosthetic hand. It defines the motion of the fingers in the prosthesis using a combination of EMG and computer vision. In this module, the system classifies the contractions made by the user into three commands: one to take a picture, one that can be used for selecting an interaction or trigger command, and one to cancel the operation or to refuse an interaction suggestion. The system can distinguish the correct command based on the current state of the state machine that manages the behaviour of the interface. Table 9 shows the type of contraction associated with the commands.

The interface works as follows: the user sends a simple command using the EMG sensors (first contraction in Figure 25) to take a picture of the object they want to interact. , and then a label of the object is returned (in this case, "mouse"). The system then searches for this object in the database dictionary and the corresponding grasps associated with it and suggests to the user which interaction is more likely correct to interact with the object in the image. The users can either accept or reject the suggestion with commands from the



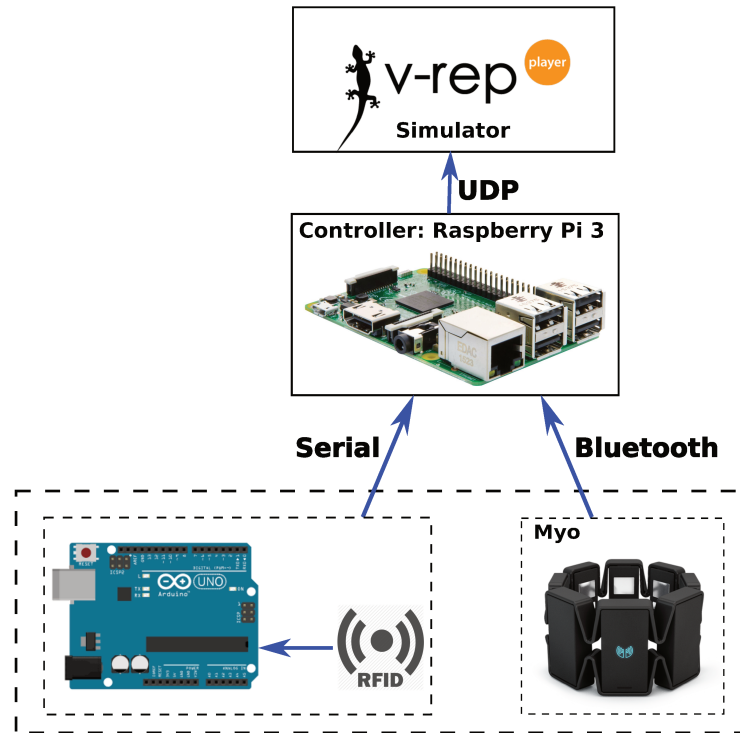





Figure 24 – RFID module communication diagram.

Table 9 – Contraction and command association.

Command	Representation	Function
Fist		Take a picture
Wave out		Refuse suggestion Cancel operation (return to relaxed hand)
Wave in		Accept suggestion Trigger

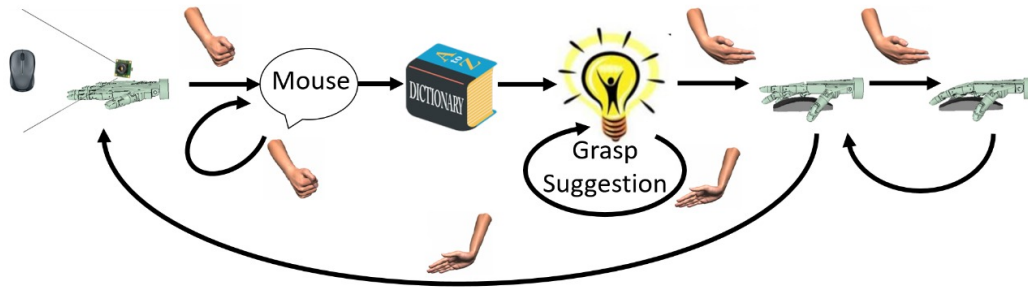


Figure 25 – Vision module overview.

EMG sensors. When the users refuse the interaction offered by the system, the system shows the next probable one until the user finds the interaction that better suits the task he wants to perform. This process is shown on Figure 25.

The architecture of the vision module is illustrated on Figure 26. The EMG signals are processed the same way it happens in the other modules (see section 3.2). For this module, three different contractions are needed as buttons to take a picture, validate a proposed interaction, send triggers to the prosthetic hand, refuse a proposed interaction, and to cancel an operation.

The other input of this module is the image acquired by the camera. When the system perceives the contraction to take a picture of an object, the picture is taken and sent to be processed. One label defining the object present in the image is returned to the system, and the process of grasp suggestion to the user starts. When the user accepts one suggestion, the *Controller* sends the interaction number to the virtual prosthesis in V-REP (as in Table 2). The detailed workflow of this module is shown in subsection 3.5.1.

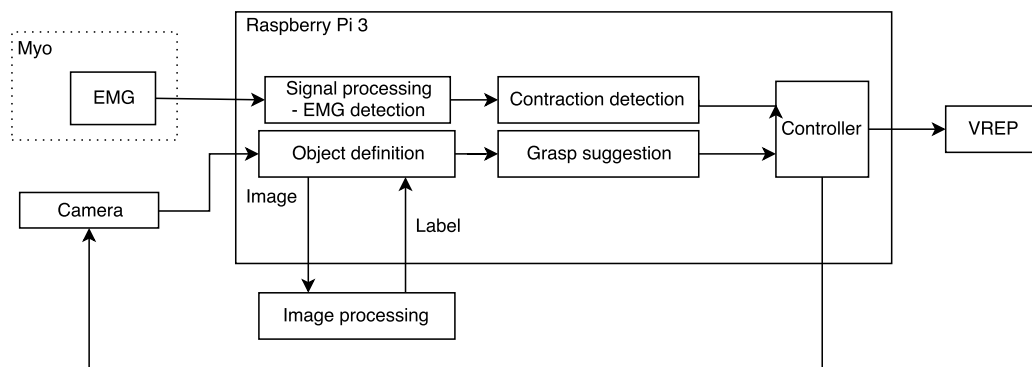


Figure 26 – Vision module architecture.

### 3.5.1 Workflow of Vision Module

To better understand the vision module, the system is divided into four parts – the user, the Central controller, the image recognition algorithm, and the database (see Figure 27). When the user put on the Myo, the prosthetic device goes to the relaxed hand position. Every time the user contracts his muscles, the system checks to see if it is a command to take a picture of an object. Whenever this is true, the camera will be initialised, and the picture is taken and sent to the image recognition algorithm to process this image.

The algorithm will process the image and return the name of the object that is prevalent in the image. When the label is valid (that is, when it describes a real object), a search is conducted in the database to check which sequence of interaction will be suggested to the user. To define this sequence, each object that a user already interacted with is associated with one or more types of interaction through a weight that ranges from 0 to 1, representing the percentage of use of the grasp with the related object. In this structure, 0 means that the user never used the grasp in the list to interact with the object while 1 means that the user chose that grasp 100% of the time.

After the first suggestion, if the user does not accept it nor take a new picture, the next most used interaction to the object is suggested. When the user accepts the suggestion made by the system, it will be checked if the object already exists in the database. If so, the database is updated with the new calculation of the weight of interaction for the object. If not, the new object is added to the database along with the chosen interaction.

When an object is seen for the first time, all the possible interactions have the same weight (0). Therefore, a default order of interactions is suggested based on the most common ones used according to Kapandji (2000).

After the user chooses the interaction, the position of the fingers in the prosthetic hand is sent to V-REP. From there, the user can cancel the interaction or send a trigger command when the interaction allows subactions (for example, the click of a mouse).

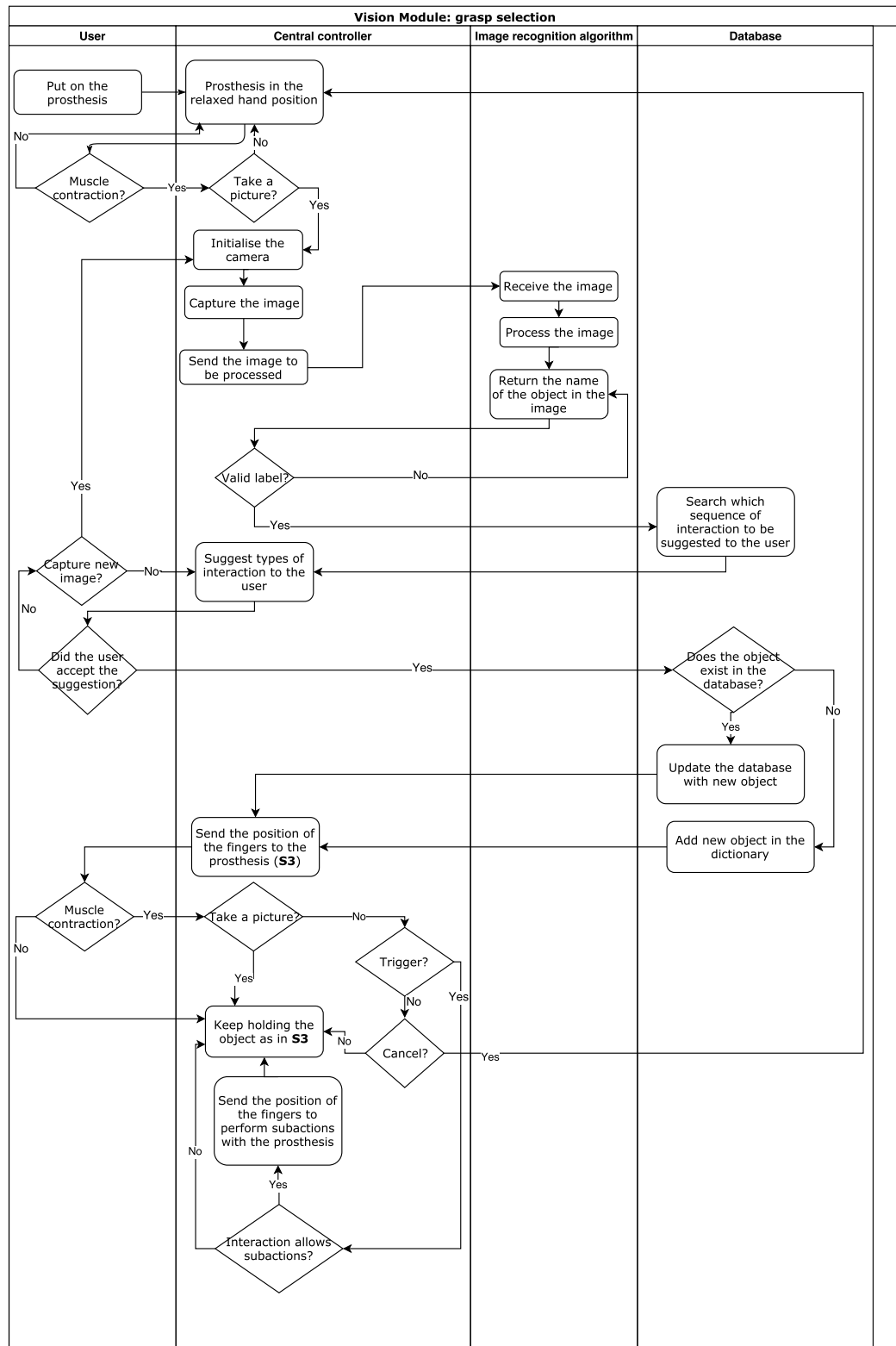


Figure 27 – Vision module workflow.

### 3.5.2 List of Materials

The materials listed on Table 10 were used to build the vision module interface. The camera used was a Camera Module V1 for Raspberry Pi. Its specifications are listed in Table 11. Hardware and software features of the camera can be found at Raspberry Pi Foundation (201-).

Table 10 – List of materials to build vision module

Material	Quantity
Raspberry Pi 3 model B	1
Camera Module V1	1
Myo armband	1
Myo bluetooth adapter	1
LCD display 16x2	1
Red LED 5 mm	1
Green LED 5 mm	1
Resistors 1 k $\Omega$	2
Potentiometer 10 k $\Omega$	1

### 3.5.3 Schematics

As explained, this interface suggests to the user some types of interactions in the form of text (i.e., power grip, and tripod grip). For the user to be able to see this suggestion, it is necessary that the prosthesis has an LCD that shows the text to the user. Therefore, as for the motion interface, a PCB prototype of the visual feedback offered to the user was built for the vision module, and it is shown in Figure 28.

When the picture of the object is processed, the suggestion is showed in the LCD. Every time the user rejects the suggestion, the next one will appear in the place of the previous one. When the user accepts the suggestion, the confirmation LED (green) turns on, and the interaction is sent to be seen on VREP. When the user finishes and wants to go back to the relaxed hand position, the user performs the cancelation contraction, the red LED turns on, and the prosthesis in the simulation goes back to the relaxed hand position.

The schematic used to build the PCB is illustrated in Figure 29. In this figure, DS1 is the LCD used, RED1 is the red LED to inform cancelation of commands, GREEN1 is the green LED to inform confirmation commands. Device P2 is the Raspberry Pi 3, RV1 is the 10 k $\Omega$  trimpot, and R1 and R2 are the resistors. It is important to highlight that the LCD operates at 5 V while Raspberry Pi 3 operates at 3.3 V. However, as the data pins are in the write mode, meaning that the information is going only in one direction (from the Raspberry

Table 11 – Technical hardware specifications for the Raspberry Pi Camera Module.

Camera Module V1	Technical specification
Size	25 x 24 x 9 mm
Weight	3 g
Resolution	5 Megapixels
Video Modes	1080p30, 720p60 and 640x480p60/90
Linux integration	V4L2 driver available
C Programming API	OpenMAX IL and others available
Sensor	OmniVision OV5647
Sensor resolution	2592 x 1944 pixels
Sensor image area	3.76 x 2.74 mm
Pixel size	1.4 $\mu\text{m}$ x 1.4 $\mu\text{m}$
Optical size	1/4"
Full-frame SLR lens equivalent	35 mm
S/N ratio	36 dB
Dynamic range	67 dB @ 8x gain
Sensitivity	680 mV/lux-sec
Dark current	16 mV/sec @ 60 C
Well capacity	4.3 Ke-
Fixed focus	1 m to infinity
Focal length	3.60 mm +/- 0.01
Horizontal field of view	53.50, +/- 0.13 degrees
Vertical field of view	41.41 +/- 0.11 degrees
Focal ratio (F-Stop)	2.9

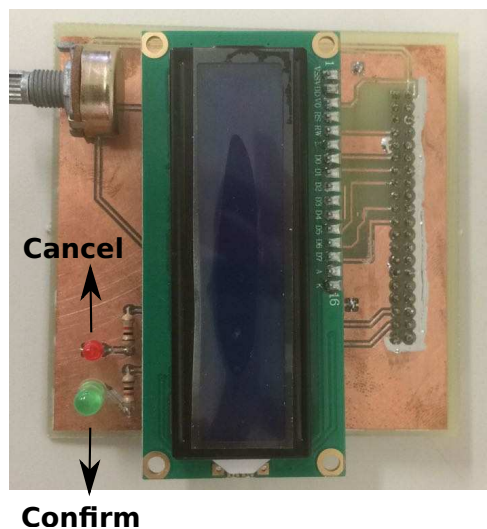


Figure 28 – Vision interface feedback prototype.

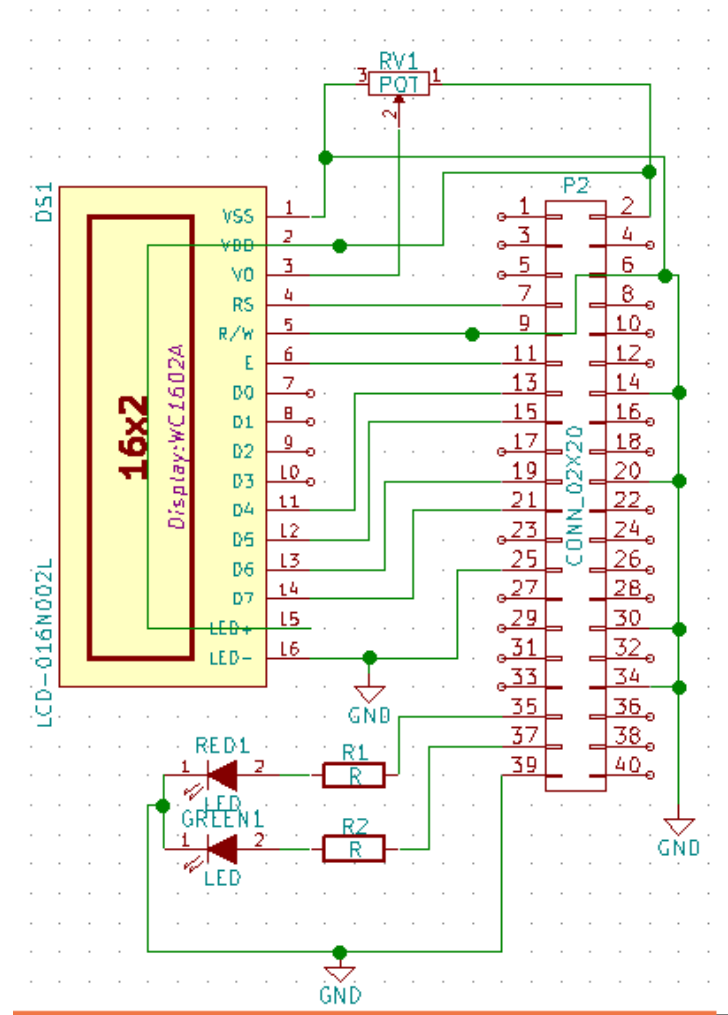


Figure 29 – Vision interface feedback schematic.

Pi 3 to the display), there is no risk in burning the General Purpose Input Output (GPIO) used on the Raspberry Pi.

### 3.5.4 Communication Architecture

To communicate the peripherals in this module to the controller different protocols and buses were used, as can be seen in the communication diagram showed in Figure 30. The two sensors that work as the input of the vision interface are the EMG sensors embedded in the Myo and a camera. The Myo sends the electrical activity of the muscles of the user to be processed in the controller through Bluetooth.

Since we used a Raspberry Pi 3 as the controller, it has a specific bus to communicate with the Camera Module – the Camera Serial Interface (CSI). This is because the camera module is intended to be used only with the Raspberry Pi, and it has two data lanes. One

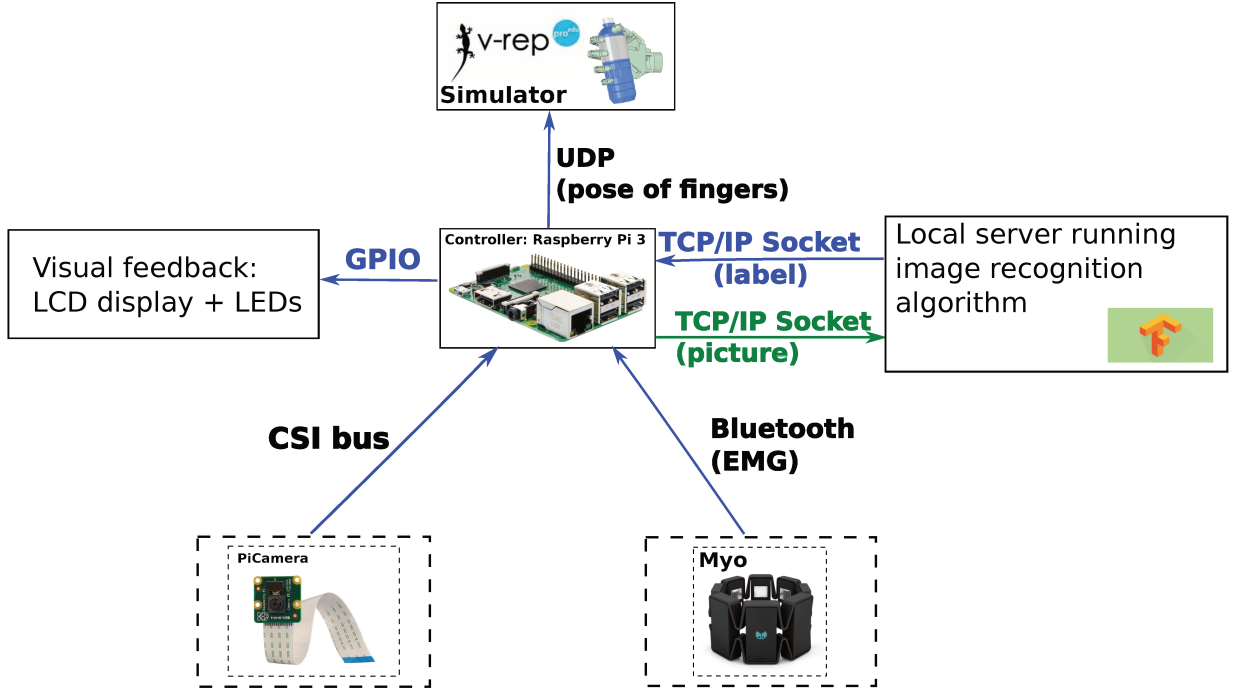


Figure 30 – Vision interface communication diagram.

data lane is for the transfer of clock signals and data to the processor while the second data lane is for SCL/SDA lines that is a bidirectional control link. This schema can be seen on Figure 31, where  $N$  is 2 for the Raspberry Pi 3 bus.

For the prototype, a local server with TensorFlow installed was necessary to process the images since the processing time of the Raspberry Pi 3 running the image recognition algorithm was not suitable for an embedded application. Therefore, the controller sends the image through a TCP/IP socket, the server receives it, process and sends back to the controller with the label describing the image. For implementation in a real prosthesis, two approaches can be chosen to replace the need for a server. The first one is the use of a smartphone to run the image recognition algorithm. The second one is the use of a more powerful controller than the Raspberry Pi 3 (such as Dragon board from Qualcomm). Moreover, the image recognition algorithm can be optimised to run into the Raspberry Pi 3 at a faster speed.

The system also has a feedback module, composed of the LCD and LEDs as seen in the previous section. These peripherals communicate to the controller using the GPIO ports of the Raspberry Pi 3 as seen in Figure 29. Finally, through a UDP protocol, the controller sends the position of the fingers of the simulated prosthetic hand to V-REP.

In a further approach still under development, the local server is replaced by an application in a smartphone. Due to its computational power, the smartphone will serve



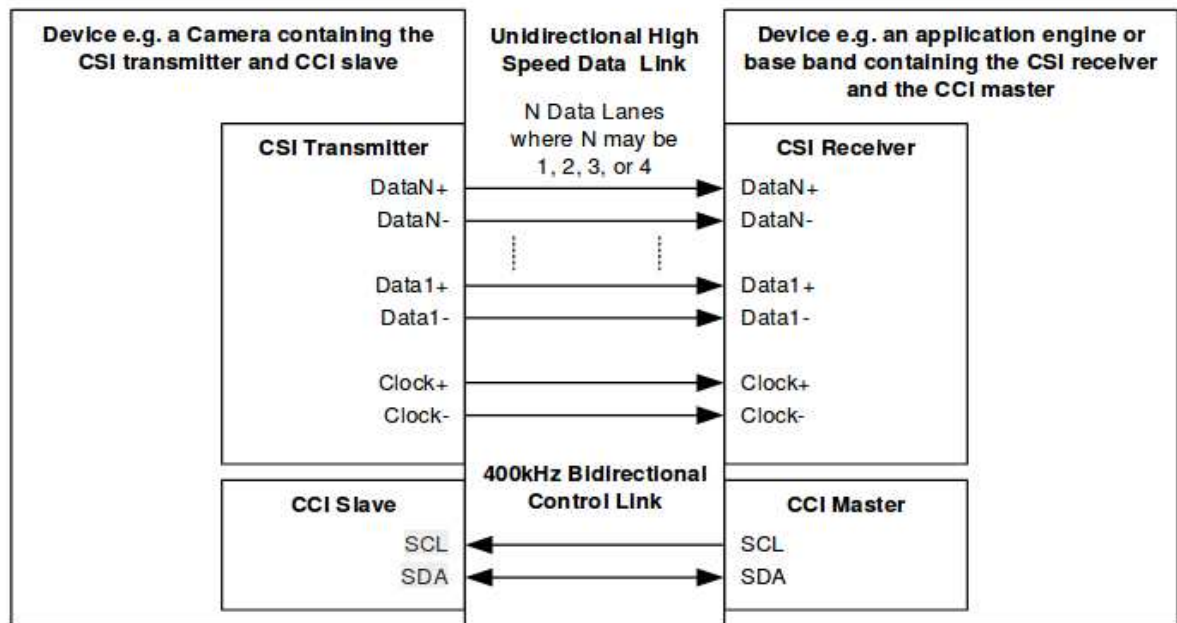


Figure 31 – CSI-2 and CCI Transmitter and Receiver Interface.

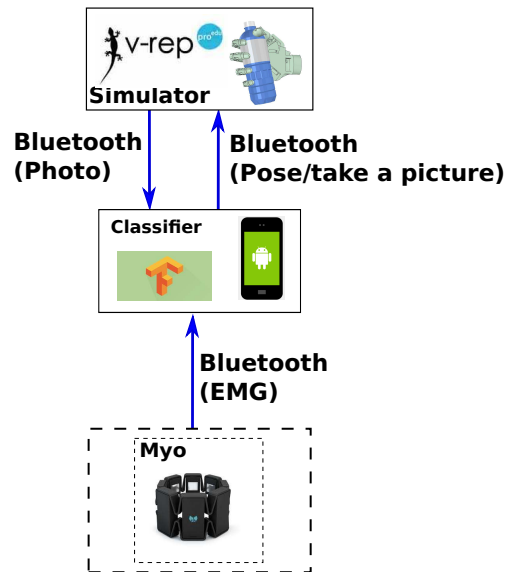


Figure 32 – Communication architecture of the vision module with a smartphone.

as the controller of the system instead of the Raspberry Pi 3. This way, it will hold the massive lifting computation required by the image recognition algorithm and the classification algorithm of the EMG signals. Figure 32 shows the communication architecture of the next version of the Vision Module. However, this work presents only the results of the Vision Interface with the Raspberry Pi 3 as the controller.

## 3.6 Procedures

In this section, the NASA Task Load Index evaluation will be described as well as the environment where the tests with the interfaces explained previously took place.

### 3.6.1 NASA Task Load Index (NASA-TLX)

NASA Task Load Index is the evaluation we are using to compare the modules developed. It is a procedure developed by the Human Performance Group at Nasa Ames Research Center that aims in collecting the overall workload score of a task and it is based on six scales being Mental Demand, Physical Demand, Temporal Demand, Performance of the volunteer during the task, Effort, and Frustration. The weighted average of these scales provides the workload of the specific task performed by the user. This weighted average is calculated based on the personal importance to the raters for each of the six scales. These scales provide data to analyse whether or not one interface is easier to use and why.

The evaluation using NASA TLX happens in two parts – the raw ratings of the scales (magnitude of load) and the source of workload (weight). For the first one, the raters are given a rating sheet containing the six scales presented as a line, divided into 20 intervals of 5 in 5 units, being the limit descriptors "Low" (0) and "High" (100). The subjects have to mark each scale in the location that they believe suits the best for the task they were asked to perform. According to NASA (2011), this step of the test may happen during or after the task. The rating sheet given to each volunteer during the tests is found in Annex A.

For the source of workload, the raters evaluate the importance of each scale for the specific task. That means, they will evaluate which scale contribute the most to the source of workload for the task they were asked to perform. There are 15 comparisons of the scales, and each pair was presented as a card to the volunteers. For each rater, the pairs were presented randomly and individually. The number of times that each scale is marked is the weight each factor contributes to the workload, and it ranges from not relevant (0) to more important than any other (5). This way, it is important to realise that, in the case of one of the scales is marked five times, no other scale can be marked five times. Figures 33 and 34 depicts an example of how these cards were arranged.

After gathering all the information necessary, the weighted average of each task is calculated according to Equation 3.4, where the Adjusted Rating is the raw rating of each scale multiplied by its weight, and 15 is the number of possible comparisons using the six

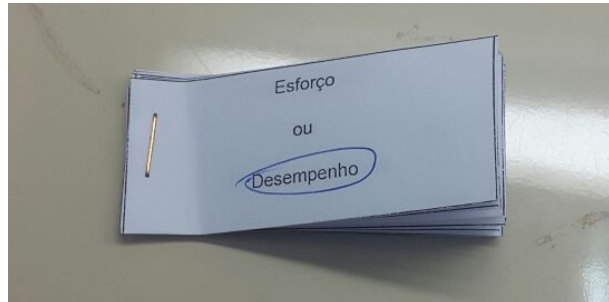


Figure 33 – NASA TLX comparison cards.

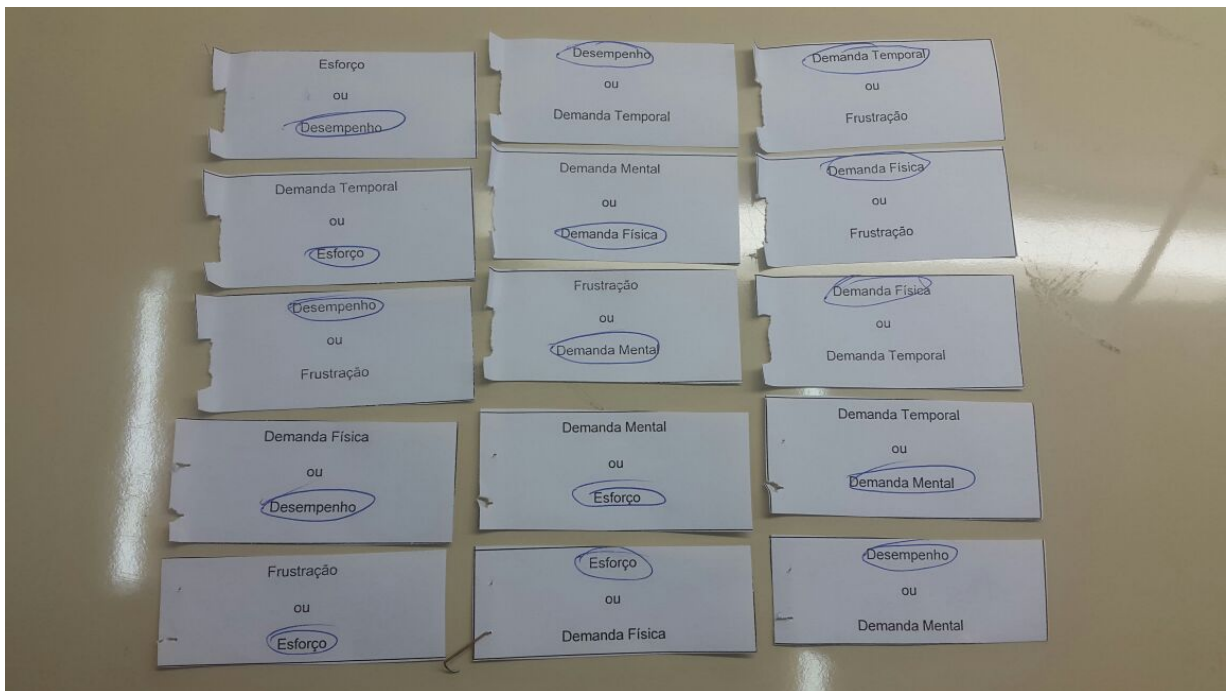


Figure 34 – NASA TLX comparison cards detached.

scales evaluated in the test.

$$\text{Weighted rating} = \frac{\sum \text{Adjusted Rating}}{15} \quad (3.4)$$

### 3.6.2 The Environment of the Test

Due to the fact that we could not find within the university community of Campinas a voluntary amputee to carry out the necessary tests for the evaluation of the interfaces, the tests were conducted in two laboratories – the Laboratory of Computer Engineering and Industrial Automation (LCA) in the State University of Campinas (UNICAMP), and the Laboratory of Instrumentation and Biomedical Engineering (LIEB) at Sao Paulo State

University (UNESP) campus Ilha Solteira – during November of 2017.

In both laboratories, the volunteers were accompanied by the researcher responsible for the test, in a quiet room, without disturbances to assure they were in a comfortable environment while testing the interfaces. The amputee required the presence of a person of his trust in the laboratory during the tests to help him in case he needed and to make him feel more comfortable.

To reach reproducibility in the tests, all of them followed a pre-defined script. First, the participants provided written consent to take part in the experiment, which was approved by the Ethical Committee of the University of Campinas (Brazil) under the CAAE number 58592916.9.1001.5404 (see Appendix A). Then, the researcher had to fill out the form of participation of the volunteer, which had questions about the volunteer such as age and gender (see Appendix B).

After that, the researcher was to explain how the interface to be tested was going to work and what tests the user was going to do. After the explanation, the experiments began. First, the calibration of the armband was conducted. The calibration was made using the Myo armband software.

Following the calibration of the armband, a quantitative test was conducted. In this test, the goal was to analyse if the orientation of the arm had some influence on the classification result of confirmation and cancelation contractions. The volunteers had to perform cancelation and confirmation contractions in 5 (five) different orientation with the arm extended and not extended.

After that, the task the volunteers had to perform were presented, as well as instructions about how to select each interaction necessary to complete the tests. The description of each task can be seen in Table 12.

As NASA (2011) suggests, the volunteers had between 5 and 10 minutes to get familiar with the system. Then, the volunteers had ten trials to test the interface, however, as stated in the approval, they could stop at any time, and most of the volunteers made only up to 5 trials.

During these trials, the researcher calculated the time the volunteers took between starting the selection and the end of the interaction. The goal of this test is to compare the mean time necessary to complete a task with healthy people using the simulation and the time necessary to complete a task with an amputee. This is important to analyse whether the contractions required by the system are simple to be done for transradial amputees.

After the trials, the volunteers were asked to evaluate the interface using the rating

Table 12 – Interactions performed by the volunteers during the tests.

Interaction	Description of the task
Power grip	<ol style="list-style-type: none"> <li>1. Select the interaction</li> <li>2. Hold a mug (simulation)</li> <li>3. Cancel command (relaxed hand)</li> </ol>
Finger point	<ol style="list-style-type: none"> <li>1. Select the interaction</li> <li>2. Point the finger (simulation)</li> <li>3. Cancel command (relaxed hand)</li> </ol>
Mouse grip	<ol style="list-style-type: none"> <li>1. Select the interaction</li> <li>2. Hold the mouse (simulation)</li> <li>3. Interact with it (send triggers to simulation)</li> <li>4. Cancel command (relaxed hand)</li> </ol>
Tripod grip	<ol style="list-style-type: none"> <li>1. Select the interaction</li> <li>2. Hold the pencil (simulation)</li> <li>3. Cancel command (relaxed hand)</li> </ol>

sheet presented in Annex A. Right before the evaluation, they got an explanation of what each of the scales meant according to NASA (2011).

Next, they evaluated the source of workload (the weight of each scale) using the individual cards as presented in Figure 33. Also, they were asked whether or not they would like to provide any further information about their experience through a small questionnaire presented in Appendix C.

To avoid muscle fatigue, most volunteers tested one interface per day. The ones who had less time available tested two or three interfaces on the same day but with 5 minutes break among tests with different interfaces to not overburden the muscles.

### 3.7 Summary of the Chapter

This chapter presented the methodology used to develop and evaluate the three interfaces to control a prosthetic hand. First, the scene in the V-REP simulator used to represent the prosthetic hand was described as well as the different movements the prosthetic hand can perform. Then, it was explained how the Myo armband is used to acquire the EMG signals that work as one of the inputs of the three interfaces. The software and hardware requirements of each module were also detailed to make sure others can reproduce this work. Finally, the full experimental procedure used to test and compare the three modules was

described.

## 4 Results and Discussion

The goal of this chapter is to bring the evaluation of the results of the tests described in chapter 3. Twenty-one (21) volunteers, one of who is an amputee, were invited to test the three modules developed for this project. The social profile of the volunteers is described, along with the medical characteristics of the amputee in section 4.1. In section 4.2, the results of the NASA Task Load Index for healthy subjects are described. Followed by section 4.3, where the amputee's results of the tests are presented. After the analysis of each module's score in the tests, it will be presented a comparison among them to highlight their advantages and disadvantages.

### 4.1 Social Profile of Volunteers

Table 13 shows an overview of the volunteers who tested the modules described in chapter 3. Of the 21 volunteers, 14 were male, and 6 were female with the range of age from 20 to 55 years old. One of those volunteers was a male amputee. Table 14 shows the identifiers of the healthy volunteers, their gender, age and level of education. It is important to mention that for personal reasons, not all healthy volunteers tested the three developed modules; most of them tested all modules while some could only evaluate one or two modules. Therefore, all graphs in this section specify which volunteer tested each module.

The information regarding the amputee volunteer is showed on Table 15. The volunteer is a 51 years old man, 16 of which being an amputee because of an accident. His missing limb is the left arm, but this is not his dominant side. The level of his amputation is transradial, and he has approximately 19 cm of the residual limb. He tried to use a myoelectric prosthesis after the accident, but after two weeks he started feeling pain on his shoulder due to the weight of the prosthesis and gave up wearing the prosthetic device after six months.

Table 13 – Information of volunteer's – summary.

Male	Female	Range of age (years)	Healthy	Amputee
15	6	20-55	20	1

Table 14 – Non-amputee volunteer’s information.

Identifier	Gender	Age	Level of education
A1	M	29	Post-secondary
A2	M	25	Post-secondary
A3	M	22	Post-secondary
A4	M	54	High-school
A5	F	30	Post-secondary
A6	F	26	Post-secondary
A7	M	55	Post-secondary
A8	F	25	Post-secondary
A9	M	26	Post-secondary
A10	F	26	Post-secondary
A11	M	34	Post-secondary
A12	M	28	Post-secondary
A13	M	25	Post-secondary
A14	F	28	Post-secondary
A15	M	25	Post-secondary
A16	F	20	Post-secondary/incomplete
A17	M	35	Post-secondary
A18	M		Post-secondary
A19	M	22	High-school
A20	M		Post-secondary

Table 15 – Amputee volunteer’s information.

Identifier	Gender	Age	Level of education	Cause of amputation	Years since amputation	Missing limb	Dominant side	Prosthesis use
A0	M	51	High-school	Accident	16	Left	Right	Myoelectric for 6 months

## 4.2 Healthy Volunteers

As stated in section 3.6, the NASA Task Load Index evaluation was conducted for all modules and volunteers. Recapitulating, this evaluation takes into consideration six scales: Mental Demand, Physical Demand, Temporal Demand, Performance, Effort, and Frustration. The first part of this test consists in collecting the raw rating for each of these scales. Figure 35 illustrates an example of evaluation of the Motion Module made by volunteer A1 during his tests.

One can observe that according to him, the interface requires more mentally (60) than physically (25) from the user; and more Temporal Demand (80) than any other scale. It means that this volunteer suffered less physical wear during the task than mental wear, which is justified by the fact he had to remember a pattern of contraction-direction to select



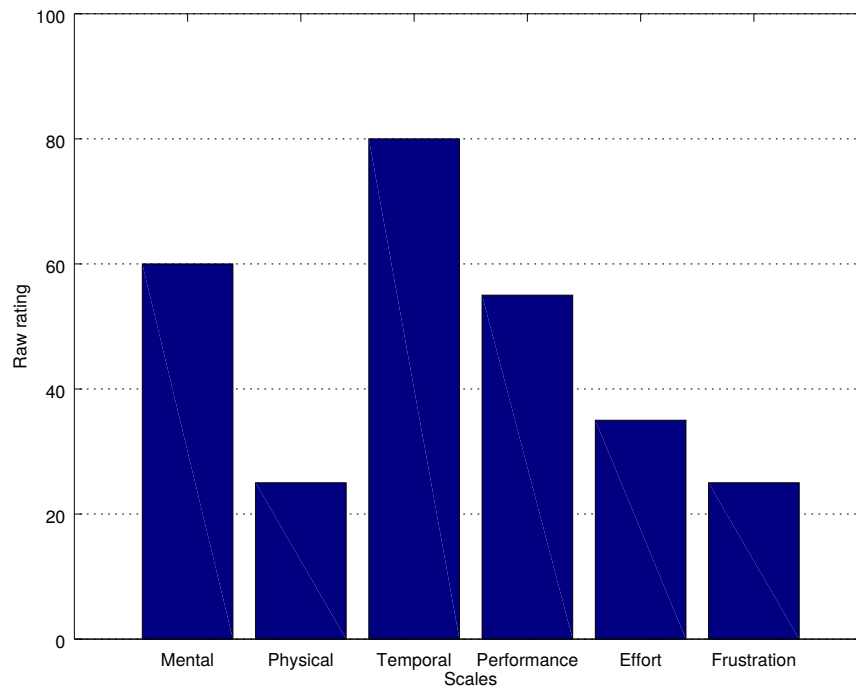


Figure 35 – Example of rating the scales for Nasa Task Load Index evaluation by a healthy subject. The range of the scale varies from 0 (low) to 100 (high).

an interaction in the prosthetic hand during the tasks. From Figure 35 it is also essential to analyse the overall Performance of the user while carrying out a task, in this case, 55 out of 100, which means he does not entirely fail but neither was he very successful accomplishing the goals of the tasks. To achieve this value of Performance, he did not have to work very high (35 out of 100 in the effort scale) and his Frustration while using the module was also low (25 out of 100).

The second part of the NASA TLX evaluation is to choose which scale has more weight for the calculus of the overall workload of the test by completing the card comparison of the scales. After this step, one found that the volunteer A1 had an overall workload of 56/100 using the Motion Module. Further tests using the RFID and Vision Module showed the user had an overall workload of 9 and 18 respectively. Meaning that A1 had less cognitive effort using the RFID Module, Vision Module, and Motion Module, respectively.

However, one person's perspective is not enough to assure how the modules are compared. Consequently, tests with more volunteers were conducted. Subsection 4.2.1 to subsection 4.2.3 shows the raw rating for all the volunteers who tested the modules. Subsection 4.2.4 shows the overall workload calculated for each module for all the volunteers.

### 4.2.1 Motion Module Analysis

Figure 36 and Table 16 show the raw rating evaluation and the mean and standard deviation of each scale evaluated by Nasa TLX, respectively.

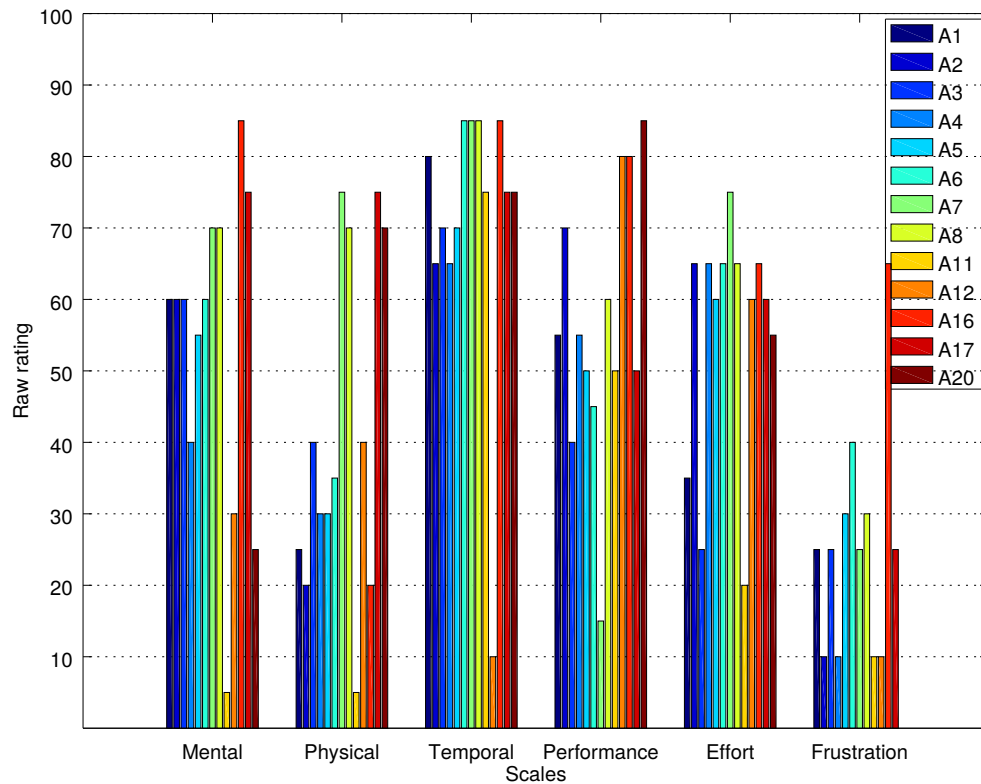


Figure 36 – Motion module: raw rating.

Table 16 – Values of mean and standard deviation (SD) of each scale analysed in Nasa TLX for the Motion module.

Scale	Mean $\pm$ SD
Mental demand	53.462 $\pm$ 22.489
Physical demand	41.154 $\pm$ 23.643
Temporal demand	71.154 $\pm$ 19.807
Performance	56.538 $\pm$ 19.081
Effort	55 $\pm$ 17.078
Frustration	23.462 $\pm$ 16.756

The first thing to observe in the graph is that the variation on the rating is considerably high for all the scales. Table 16 shows a standard deviation of 16.756 for Frustration and 23.643 for Physical Demand; meaning that the values of all scales tend to be far from the calculated mean. The factors that influence the experience of the user do not come only from the task itself, but also from their feelings while performing the task. Consequently,

these rates are subjective and the variation when rating the scales is expected since what will define the overall workload of the tasks is the combined value of the raw ratings and their respective weight for each volunteer.

For the tasks using the Motion Module, the rates of Mental Demand were expected to be high since the volunteers would have to memorise the correct combination of contraction-direction necessary to complete the tasks, demanding from the users to memorise four patterns to select a grasp in a short period. However, the outcome of volunteers A8, A11 and A20 surprised in the sense that they rated the scale as low mentally demand.

They affirmed that as soon as the patterns finished in a position where they could imagine how to grasp the objects, it would be easy to memorise the right combination. However, what they felt most uncomfortable was the time they need to respect to confirm a combination and the time interval between contractions since sometimes they would contract a muscle and the system would not perceive it as a command due to the time limit between contractions. One of the volunteers stated that this behaviour of the system confused him, increasing the effort since he had to concentrate more on respecting the timing of the system than memorising the combinations of contraction-direction.

The variation in Physical Demand is explained since some volunteers considered 3-4 contractions to select a grasp too much contractions (even though did not feel muscle fatigue) while other subjects did not consider that the module demanded too much physically since they did not feel muscle fatigue.

Temporal Demand had the lowest variation compared to the other scales. The majority of the subjects (12/13) rated this scale between 65 and 85, meaning that they felt time pressure while performing the tasks; except for subject A12, who had a different perception of the time component of the test, rating the scale as low time demanding (10/100). Since the majority of the volunteers felt time pressure due to the rate at which the task occurred, this module needs improvements so the users will not have to obey a period to complete a task. Also, some users indicated that after using this module for some time and memorising the sequence of directions and contractions to activate a grasp, they needed less time to perform the required combination. For this reason, the time between contractions should adapt to the rhythm of each user using the interface.

Regarding the Performance of the volunteers executing the tasks and the Effort they had to do to reach that performance, one can observe that the subjects that had average Performance had to make significant Effort to reach this results. The Effort was around 55-75/100 to obtain performance ranging between 75-85/100. The calculus of mean for these scales reinforce that to have a performance of 56.538 the subjects have to make almost the

same amount of effort – 55. That implies that the Motion Module requires a significant amount of effort from the user to control the prosthesis.

The last scale showed Frustration. The mean rate for Frustration was low (23.462) with high standard deviation. We expected Frustration levels under 10 for non-amputees volunteers since they do not have limitations while performing the contractions. Nevertheless, the amount of effort these subjects had to make to reach only average Performance made the level of Frustration more significant than expected.

#### 4.2.2 RFID Module Analysis

Sixteen (16) volunteers tested the RFID Module. The results of the raw rating of this module are shown in Figure 37. The first thing to observe in this chart is the difference between the rates when compared to the Motion Module; the values of Mental Demand, Physical Demand, Temporal Demand, Effort, and Frustration are low, and their Performance in using this module is very high in average. Nevertheless, as shown in Table 17, high standard deviation within the scales is still a characteristic of the evaluation.

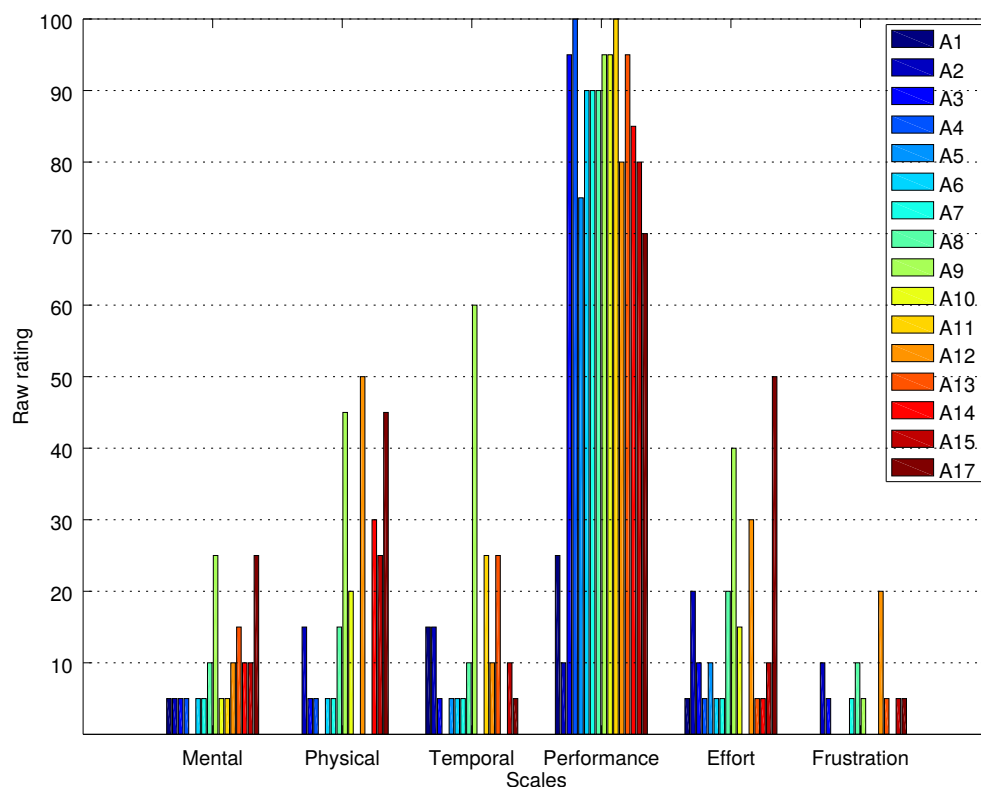


Figure 37 – RFID module: raw rating.

Table 17 – Values of mean and standard deviation (SD) of each scale analysed in Nasa TLX for the RFID module.

Scale	Mean $\pm$ SD
Mental demand	9.062 $\pm$ 7.122
Physical demand	16.562 $\pm$ 17.58
Temporal demand	12.187 $\pm$ 14.94
Performance	79.687 $\pm$ 25.914
Effort	14.687 $\pm$ 14.197
Frustration	4.375 $\pm$ 5.439

The RFID Module did not require high mental work from the users. Figure 37 illustrates that the higher score for Mental Demand was 25 with a mean of 9.062 for the 16 volunteers as showed in Table 17. This result is explained by the fact that the volunteers did not have to remember many patterns and the selection of grasps was simple to be done. As explained in section 3.4, to select a grasp using this interface, the user only needs to get closer to the object and to contract the muscles of the arm to confirm the interaction. Thus, the perceptual activity required to complete the task is low, justifying the results.

The way the module works also contributes to the low outcome of Physical Demand (16.562 on average) and Temporal Demand (12.187 on average). One contraction to confirm and one to cancel interactions avoid feeling muscle fatigue; consequently, the task ended up not being laborious for the raters. Also, this module is not time-dependent, meaning that after the user gets close to an object, he does not have to contract his muscle within a determined period. Therefore, no time pressure is felt by the user when selecting the interaction.

The average of Performance of the volunteers during the tasks using the RFID module was high – 79.687 – and the Effort required to achieve this performance was considerably low – 14.687 on average. Most participants stated during the experiment that they had to work very little to achieve their respective levels of Performance, except for A17. This volunteer had troubles while using the module because Myo did not fit appropriately in the arm. Hence the armband was frequently moving while the volunteer was trying to grasp an object (i.e., a mug during power grip test) causing many involuntary commands to be sent to the simulation.

Since the RFID interface showed to be easy to use, the volunteers felt secure while performing the tasks required during the experiment. That explains the low level of frustration rated by the volunteers on Figure 37.

### 4.2.3 Vision Module Analysis

Fifteen (15) volunteers tested the Vision Module. Figure 38 illustrates their raw rating for this module along with the values of mean and standard deviation presented Table 18. Due to the subjective nature of the test, as happened to the two other modules, the standard deviation for most scales is high.

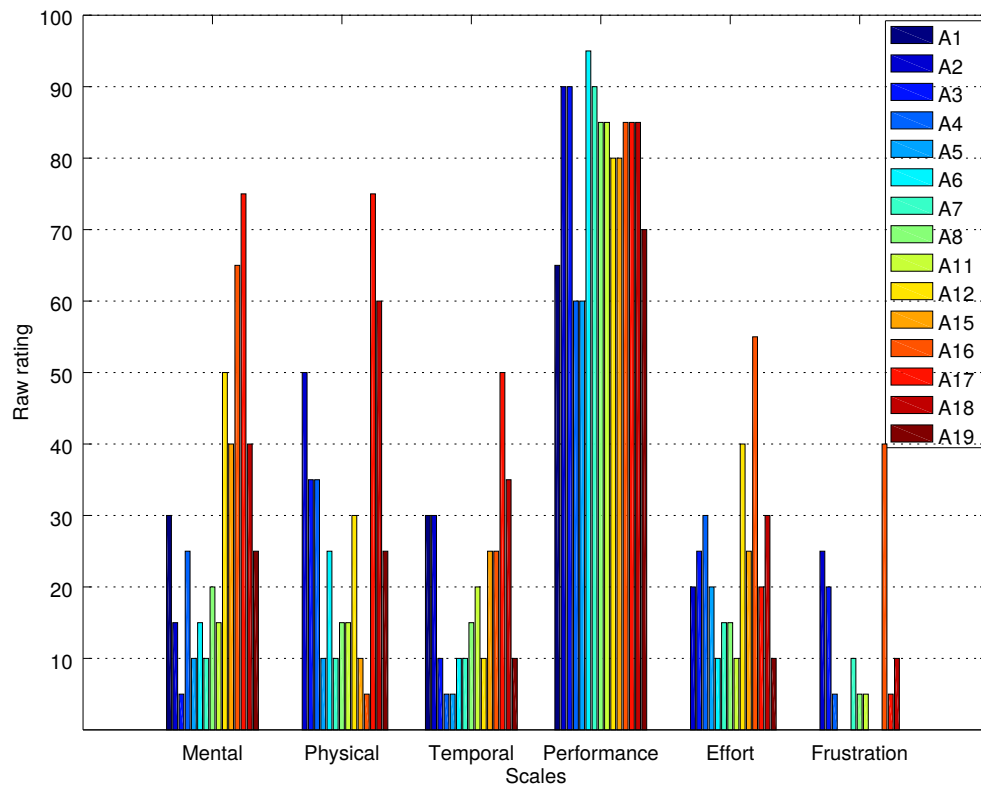


Figure 38 – Vision module: raw rating.

Table 18 – Values of mean and standard deviation (SD) of each scale analysed in Nasa TLX for the Vision module

Scale	Mean $\pm$ SD
Mental demand	29.333 $\pm$ 20.862
Physical demand	26.666 $\pm$ 21.437
Temporal demand	19.333 $\pm$ 12.938
Performance	80.333 $\pm$ 11.255
Effort	21.666 $\pm$ 13.584
Frustration	8.333 $\pm$ 11.598

In average, low Mental Demand is required from the volunteers testing the Vision Module (29.333), but as the standard deviation in Table 18 shows, values can be very distant

from the mean. This fact is observed in the chart. Most of the volunteers have indeed rated that they used very low or low Mental Demand to complete the tasks, meaning that they were comfortable and not arduous to complete (scores below 50); however, for a few volunteers (scores above 50), the task using the vision module was very mentally demanding. These volunteers often got confused about which command to make to activate the camera and take a picture of the target object (remember that three different contractions were used to take a picture, confirm and cancel an interaction).

As for the Physical Demand, the calculated average was 26.666, which is considered low Physical Demand required from the users. Similar to the Mental Demand, a few volunteers (2/15) thought that 3 or more commands were too many to complete a task especially when the interaction they wanted was not suggested within the third option. Although none of them felt muscle fatigue during the experiment, they preferred when only one or two commands were used to select an interaction.

Temporal Demand had 19.333 as average, and in the chart, it is possible to observe that all participants rated this scale below or equal to 50. Their most frequent comment regarding this scale was that sometimes the interaction they wanted was not suggested in within the third option, meaning that they had to spend a little more time choosing the desired grasp. This shows that, although the interface does not put time pressure to confirm a command as happens in the Motion Module, the time spent choosing interaction is not desirable if it is too long.

The rates for the Performance of the users were all above 60 (with an average of 80), and the average of Effort necessary to reach this result was 21.666, which is considered low. Analogous to the RFID Module, this shows that potential users can learn how to use these interfaces with a reduced training time since the volunteers who tested these interfaces were using them for the first time and only had up to 10 minutes to get familiar with the system before the experiments. Like the RFID Module, the Vision Module had a low level of Frustration mainly because the participants could complete the proposed tasks successfully.

#### 4.2.4 Healthy Subjects Overall Workload of the Modules

The chart in Figure 39 illustrates the calculated individual values of workload for each one of the modules tested by the volunteers. The x-axis shows the ID of volunteers, and the y-axis is the range of workload measured (0 to 100). It is important to emphasise that, for many reasons, not all volunteers tested all the modules developed. Volunteers A1–A8, A11, A12, and A17 tested the three interfaces; A9, A10, A13, A14, A18 – A20 tested one interface while A15 and A16 tested two interfaces. Nevertheless, their results are still meaningful to

calculate the average of the workload of all healthy volunteers who tested the interfaces.

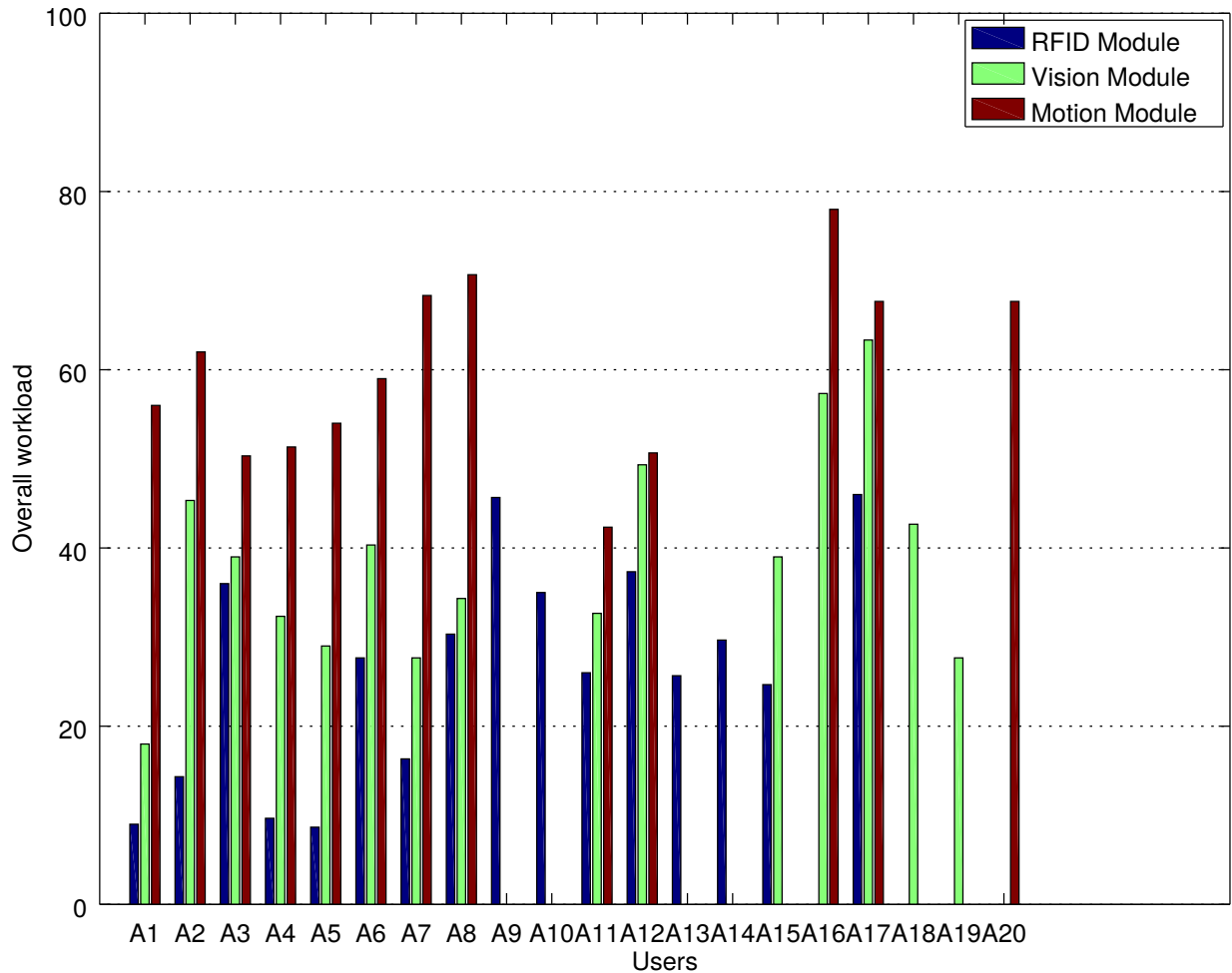


Figure 39 – Comparison of workload for the RFID, Vision and Motion modules per subject.

As the chart illustrates, the workload when using the RFID Module is lower than the workload required from the other two interfaces. All volunteers who tested the RFID Module had a workload below 50, showing the ease of use of the system in a short period. From this chart, it is also important to emphasise that the vast majority of the volunteers had a workload above 50 when testing the Motion Module. Their difficulty is mostly explained by the high Mental Demand required from the users as showed in the previous section. When analysing the weight of each scale of the task, Mental Demand has greater weight, followed by Temporal Demand, due to the characteristic of the confirmation command. Therefore, the results presented in Figure 36 for these scales contributed the most to the poor performance of Motion Module in this comparison.

For a cleaner analysis, Figure 40 depicts only the workload of volunteers who could



Table 19 – Mean and standard deviation (SD) of the workload for each module

Module	Mean $\pm$ SD
RFID	23.758 $\pm$ 12.963
Vision	37.394 $\pm$ 12.199
Motion	57.485 $\pm$ 8.928

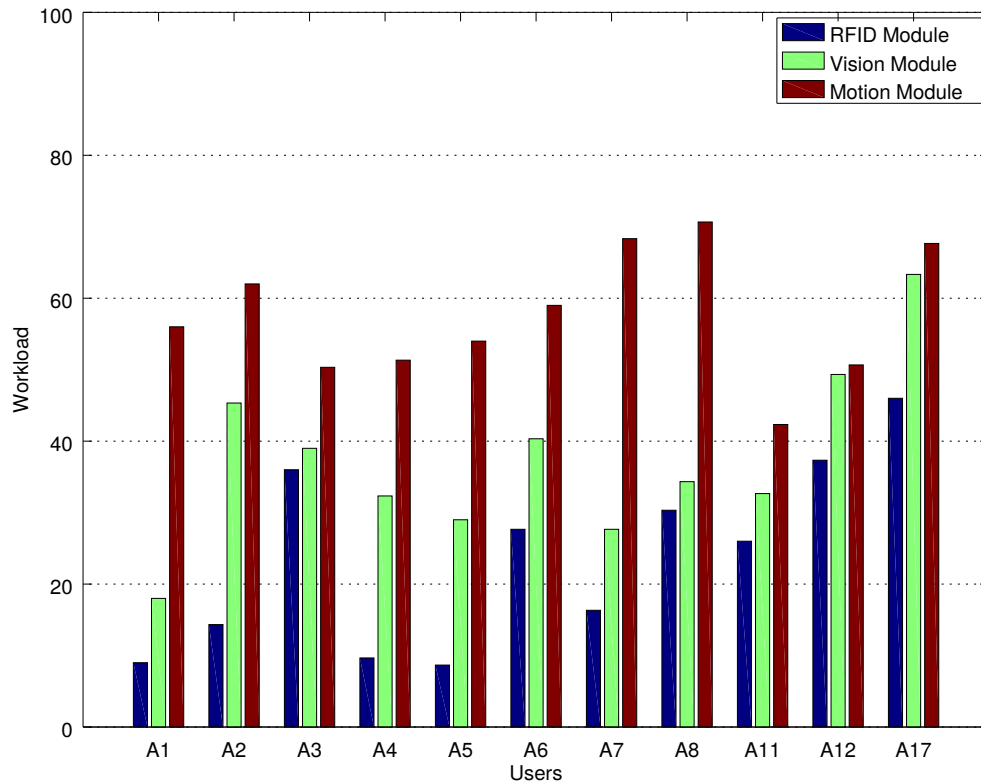


Figure 40 – Comparison of workload for the RFID, Vision and Motion modules with subjects who tested all interfaces.

test all the interfaces; along with Table 19 that shows the average of workload per module. Like the previous image, the Motion interface has the highest workload, 57.485. The low standard deviation for the Motion Module in the table indicates that although the previous section showed high standard deviation when analysing the individual scales, the outcome of the volunteers for the workload does not vary much from the mean value. Differently from the RFID Module that the value of workload from a person can vary up to 50% of the value of the mean.

The Motion Module was already expected to be the interface requiring more cognitive load from the users since it requires the user to memorise the combinations of contraction-direction, increasing the Mental Demand and Effort to reach high levels of Performance. Nevertheless, this module has advantages over the other ones. First, it is the cheapest to

be implemented from both computational and material perspective when compared to the vision and RFID Module respectively.

In addition to this, unlike the RFID Module, the Motion interface does not need all objects the user will interact with to be tagged; increasing the chances to succeed outside ideal conditions such as in the laboratory, where all objects the volunteers were testing were tagged.

As for the RFID Module, the average of cognitive load required is the lowest. The primary reason is the easiness to control the RFID interface. This interface does not require from the user to remember many combinations of movements as the Motion Module or to choose from a list of suggested interactions as the Vision Module, being indeed the most simple one to understand and to interact.

We can also observe in the graph that some volunteers, as A12 and A17, did not have a very different value of workload when compared the Motion and the Vision Module; even though the analysis of the individual scales in the previous section showed the Effort to reach their Performance lower in the Vision module. That is because, in the tests of the Vision Module, the interface did not suggest the most appropriate grasp to interact with the objects in the first place. Consequently, they had to choose from the list that sometimes showed the proper grasp lastly, increasing their effort to use the interface. However, this is a feature that can improve with the use of the interface considering that the database used to suggest the interaction will improve when more people use it, adapting itself to the needs of each user.

## 4.3 Amputee Volunteer

### 4.3.1 Motion Module Analysis on Amputee

Figure 41 illustrates the raw rating regarding the Motion Module tested by the amputee. As the figure illustrates, the module demands high levels of Mental, Physical and Temporal attention. The rates of the amputee are higher than the average of the results of the healthy volunteers, as expected. Validating what was already observed with the results of the healthy volunteers.

First, the Motion interface demands highly of the mental concentration of the user because he has to remember the combinations to select an interaction as it happened with the healthy volunteers. Besides, the user has to concentrate on the correct time interval between contractions, consequently increasing the Temporal Demand. Finally, the Effort to reach the Performance is high, meaning the amputee had to focus and perform the tasks carefully during the experiments.

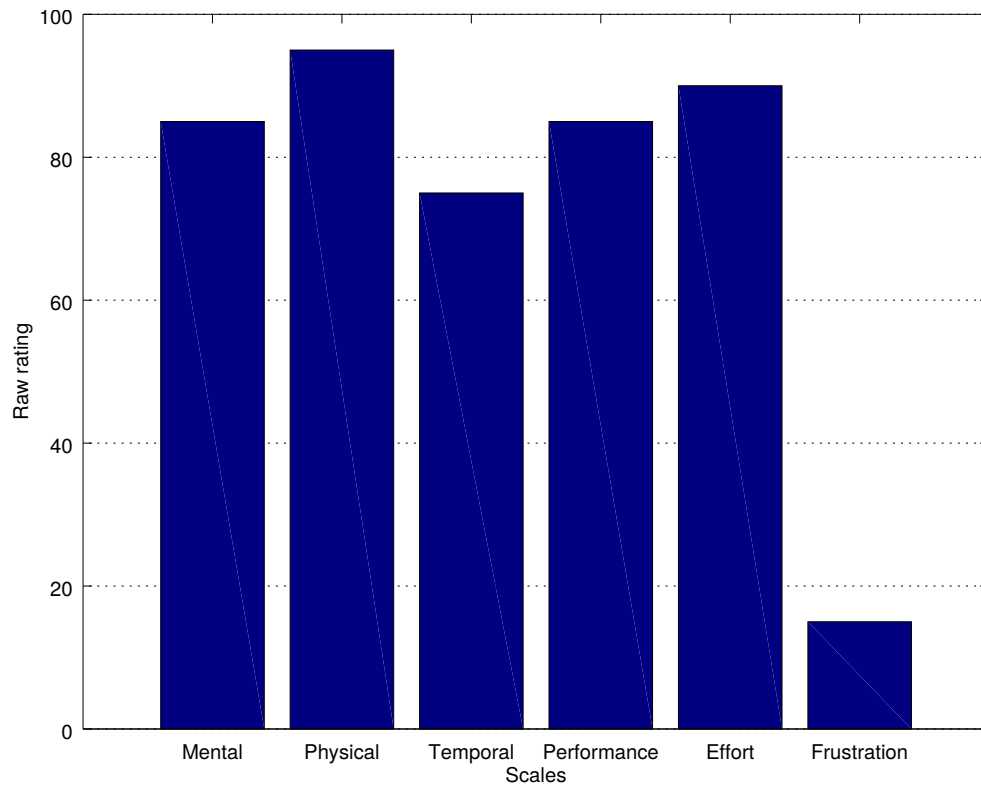


Figure 41 – Motion module: raw rating.

What was different from the results with healthy people is the amount of Physical Demand, that reached 95. According to him, the Motion Module is challenging to be used and uncomfortable due to the number of contractions he has to make to select a grasp. The interface requires too much physically from him, which makes him get tired. He also compared the Motion Module with a myoelectric prosthetic hand that he used to wear by saying that he had to make as much effort as the myoelectric prosthesis to select commands. The difference is that with the Motion Module (and the other modules as well) he does not have to dimension the contraction force and that with the modules, he could make more movements that with the myoelectric prosthesis (that only opened and closed).

The level of Frustration of the amputee user was low. One reason is that despite the high levels of Mental, Physical, Temporal Demand and Effort, the amputee could reach a high level of Performance. Meaning that with adjustments in the system, the module may get more natural for him to use.

### 4.3.2 RFID Module Analysis on Amputee

As the outcome presented for the healthy volunteers, the results of the RFID Module for the amputee show low levels of Mental, Physical, Temporal Demand and Frustration

(Figure 42). The reasons are similar to the ones explained in subsection 4.2.2: unlike the Motion Module, there is no need to memorise combinations of contractions, reducing the Mental Demand. In addition to this, using the RFID Module, the user only needs to contract his muscle to confirm, cancel or send a trigger to the prosthesis, avoiding muscle fatigue, consequently reducing the Physical Demand. The RFID Module is not time-dependent as the Motion Module, explaining the low Temporal Demand. Finally, since the user could complete his tasks with high level of Performance, his Frustration level was not high.

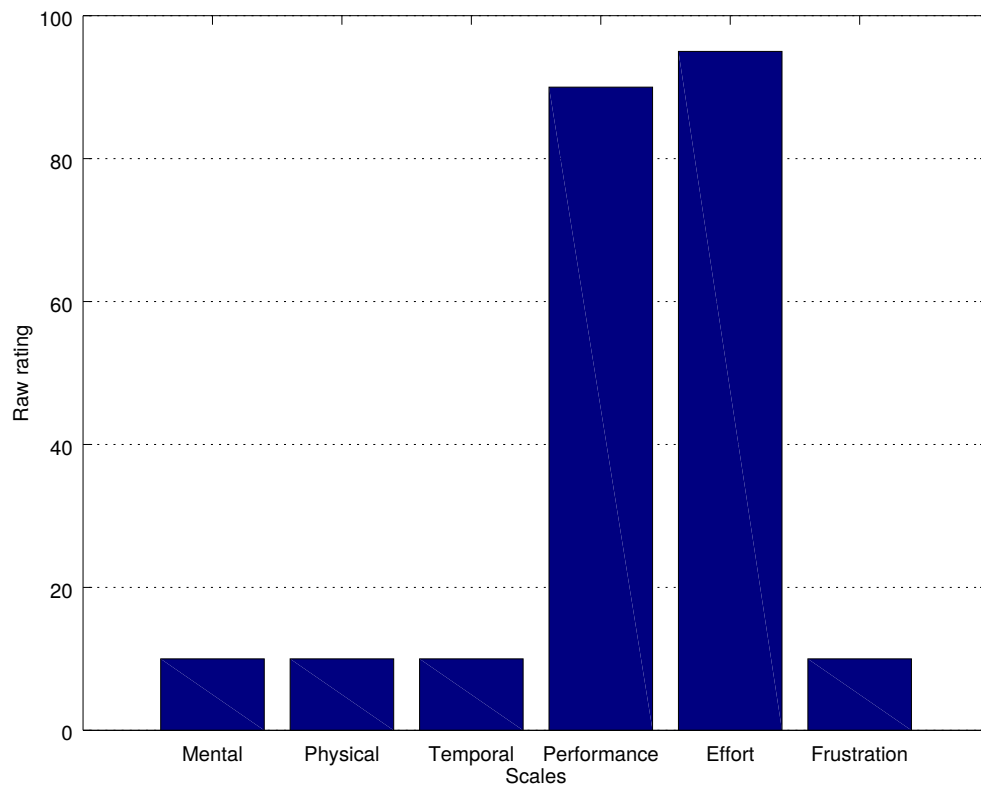


Figure 42 – RFID module: raw rating.

However, in Figure 42 one can see a significant difference from the results of healthy amputees – the Effort required to reach the Performance of the user while performing the tasks is very high, opposing to the result presented by the healthy volunteers. There is because people who are not amputee can quickly perform the contractions required to confirm and cancel the interactions (wave-in and wave-out contractions in the Myo armband classification algorithm). However, for the amputee, it was not so easy to calibrate these contractions.

The amputee was first asked to perform the movements as they appear in the Myo calibration software but he could not remember how to make those movements with his residual limb. It was like he never was able to make them in the first place. For example, we asked him to make the wave-in contraction with his right hand and then try to repeat the

movement with his residual limb, but again he could not perform it. To him, he was doing the correct movement, but the armband could feel no contraction at all.

So another approach was adopted. To control the prosthetic hand he used to have, he had to make different movements. So we asked if he could turn his residual limb to the left and right to be the confirmation/trigger and cancelation contractions respectively. Thinking of the next module (Vision interface) he would have to test, he was asked if he could make a third movement, different from the previous ones, to be a third command necessary to use with the Vision Module. When these three movements were calibrated with the armband, he could start the experiments.

According to him, if these tests were in the months right after his accident, he would probably have no trouble in reproducing the movements he had just lost. He said that in that period, he could still "reproduce" the movements of his hands because his residual limb was still responsive. In the course of time, he started to lose the ability to make specific movements with the residual limb.

Therefore, although the amputee user did not felt muscle fatigue during the experiments and his Physical Demand scale was marked as low demanding, the Effort he had to make to reach his high Performance was high, differently from the healthy volunteers.

### 4.3.3 Vision Module Analysis on Amputee

Figure 43 shows the raw ratings given to the Vision Module by the amputee volunteer. Following the tendency observed in the results of healthy volunteers, this interface required low Mental and Temporal demand from the amputee. Also, his level of Frustration using this interface was very low, and his Performance using the system was high. However, his level of Physical Demand was also high, along with the Effort required to reach his performance.

The high amount of Physical Demand comes from the fact that he had to choose from the list of suggestions offered by the system. When the first few suggestions were not the correct one, he had to keep contracting his muscles to ask for the next one. This repetitive movement made his Physical Demand higher than when using the RFID Module, but a bit lower than when he was testing the Motion Module. Notwithstanding, this is the first version of the Vision Module, and the continuous use of the system tends to create a more extensive database that leads to better and quick suggestions of correct interactions to each user.

As for the amount of Effort needed, besides the more Physical Demand required, there is still the same problem encountered in the RFID Module regarding Myo's classifier. To solve this problem, in the future implementation of both modules, a more personalised classifier can be used with the Myo. Taking away the need to perform the specific contractions the

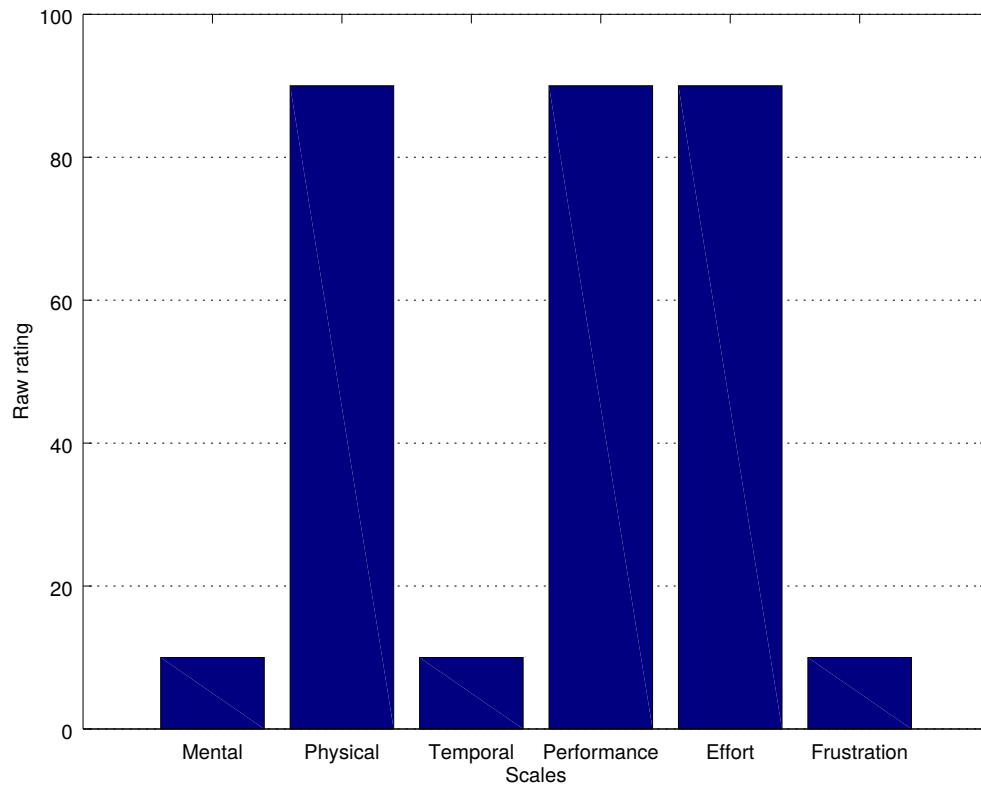


Figure 43 – Vision module: raw rating.

Myo needs to recognise a command. In the next section, the comparison of workload for each module will be presented.

#### 4.3.4 Amputee Overall Workload of the Modules

Figure 44 illustrates the calculated workload for the modules tested by the amputee. As expected from his raw rating charts and the result of the workload of the healthy volunteers, the RFID Module is the module that requires less cognitive load from the user, the Motion Module is the interface that will require the most from the user, and the Vision interface lies between the other two.

After the experiments, the amputee stated that he needed more than 10 minutes of training to control all the interfaces intuitively. However, it was enough time to perceive that the RFID and Vision interfaces were very comfortable to use in a daily basis (considering, of course, the adequate modifications in the contraction classifier, to make it easier for him to send the proper contractions). Regarding the Motion Module, his opinion was not so favorable since he felt he would have to work too hard mentally and physically to proper control this interface.

The amputee also commented that to control the myoelectric prosthesis he got after

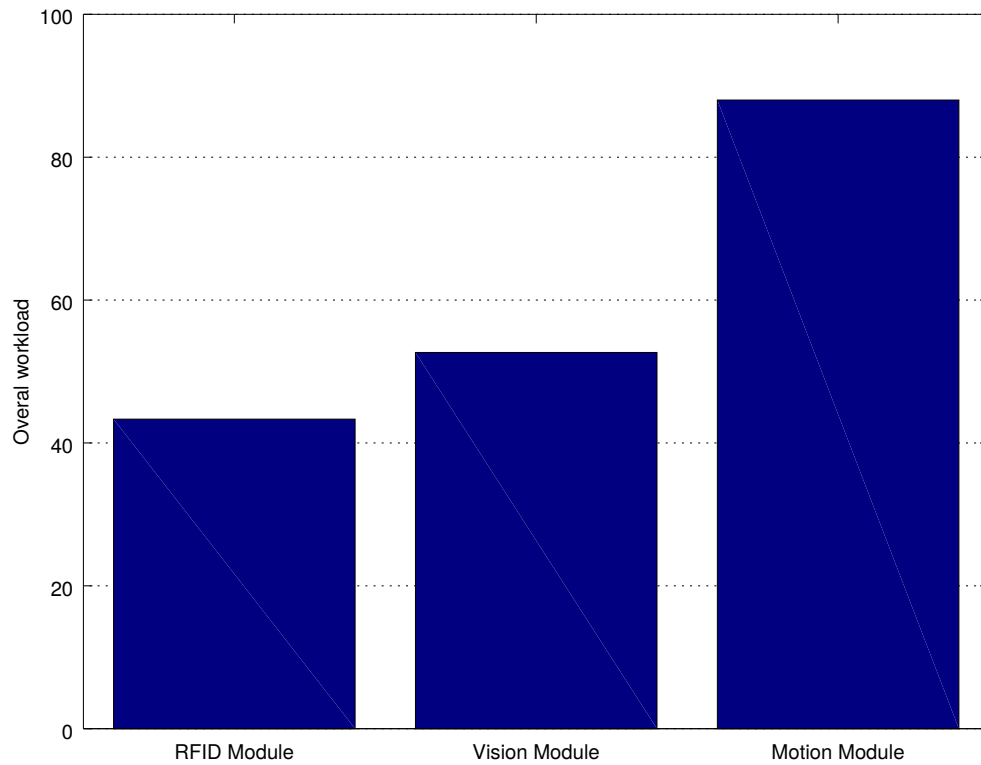


Figure 44 – Overall workload of the modules – amputee.

his accident, he had to do physical therapy for six months and that to be able to control the interfaces proposed in this dissertation in a short period with success was very exciting.

Finally, all modules presented in this dissertation have positive and negative aspects that were emphasised throughout the text. Table 20 will summarise the advantages and disadvantages of each module, giving particular focus to the comments made by the amputee regarding usability.

## 4.4 Summary of the chapter

This chapter described the results obtained from the experiments using the NASA Task Load Index evaluation. The results showed that despite the RFID and Vision interfaces are still a prototype they are a promising technology to be implemented in real prosthetic hands. To control the RFID and Vision modules less cognitive work was needed than to control the Motion interface. The latter showed itself to be very challenging to use on a daily basis due to its Mental and Physical Demand, resembling the work need to control myoelectric prosthesis that only open and close the hand. The modules, in general, need improvements, but the majority of volunteers who tested them, especially the amputee, got excited to see the interfaces implemented in prosthetic hands.

Table 20 – List of advantages and disadvantages of the interfaces proposed in this work.

Interface	Advantages	Disadvantages
Motion	Simple to implement	Users have to memorise the commands (increasing the mental demand)
	Use minimal computational resources	Resembles the physical work required by myoelectric prostheses (increasing the physical demand)
	Does not require modification in the environment	Long wait to distinguish a valid contraction (increasing temporal demand) Uncomfortable
RFID	Low mental and physical demand (requires only two different contractions to control the interface)	Limitations in non-controlled environments (requires tags on the objects)
	Low temporal demand	
	User can reach high performance using little effort	
	Comfortable	
Vision	Does not require modification in the environment	Use high computational resources
	Allows users to choose the interaction	If the database is not complete, the user has to choose from a long list of interactions (increasing the temporal demand)
	Low temporal demand	
	Comfortable	



## Conclusion

There are many works in the literature describing different types of electromyography based human-machine interfaces on controlling prosthetic devices. However, they lack evaluating the usability, comfort, easiness of control, and training time required from the users for the full control of the interface. The metrics presented are usually related to the classification accuracy of the algorithms running the interface. Also, there are commercial high-end prosthetic hands that offer advantages for amputees such as a great set of grasps and smooth movements; however, their cost makes them inaccessible for most of the people who could benefit from them. Besides, these prostheses require the user intense training to learn how to control the prosthesis, and this training is not guaranteed to be successful, leading the users to get frustrated.

In this work, three hybrid EMG based human-machine interfaces prototypes using IMU, RFID and Computer Vision were developed and qualitatively evaluated using the NASA Task Load Index to access the workload necessary to control them. This work is the result of the ongoing study on hybrid Human-Machine Interfaces for prosthetic hands to address the problem of interaction selection in those devices, not limiting to grasping. Given the characteristics of the mentioned problem, there are contributions regarding the definition of the actions the amputee can perform when using a prosthetic device and also improving the heuristic used to perform desired actions. In the first matter, the system does not limit the amputees to hold objects but allow interactions with the environment around them. In the latter, the hybrid approach of the modules intends to reduce the cognitive load required from an amputee, increasing the chances that they are going to continue using the prosthesis.

Healthy people and an amputee tested the interfaces, and the results showed that two of the interfaces (RFID and Vision Module) had higher acceptance during the tests, requiring low cognitive effort from the user to control the interfaces within 10 minutes of use. With less effort to select and trigger a grasp, users learn faster how to interact with the system, which leads them to a better experience. Despite that, the Motion Module showed itself to be more challenging to be controlled since it requires more mental effort to memorise the combinations of contraction-direction used to select the interactions, even though there is no need to measure the strength of the contraction to select the grasps as it happens in commercial myoelectric prosthetic hands.

Nevertheless, all of the interfaces have advantages and disadvantages over one another. The RFID Module, although having the lower workload required from the user to control

it, requires tagging all objects the user is supposed to interact. Therefore, the Vision and Motion Modules would be the better ones to be used in non-controlled environments. The Vision Module also required less cognitive work from the user than the Motion Module, but in early versions of this module, the user might need to spend some time choosing which interaction is more appropriate to be chosen and used with some objects. The Motion Module had the highest workload required to perform a task. However, this module is more suitable to be used in a non-controlled environment when compared to the RFID Module.

The main limitation of the work presented in this dissertation is the fact that the modules were not implemented in a real prosthetic device and the results are based in the simulation of the movements of a prosthesis that the users could see in a desktop screen. Also, the controlling interfaces need to be tested by more amputees. Since the comments from the amputee were so positive, we need to gather more insights about the time needed to learn to control the modules intuitively. Therefore, for future works, implementing the control interfaces in a prosthetic device and invite more amputees to test them using NASA Task Load Index evaluation would acquire even more relevant data to analyse the modules, improve them and release to the community.

Recapitulating this document's content, in chapter 1 the objectives, justifications, and contributions of this work were presented. Followed by chapter 2, where a review of the human hand taxonomy, types of prosthetic hands and methods proposed to control these prostheses in the literature was made. chapter 3 is dedicated to describing the methodology used in the development and evaluation of three hybrid human-machine interfaces to control grasping selection in prosthetic hands. The first technique described is called Motion Module, where the position of the fingers in the prosthetic hand simulation is changed with a combination of EMG signals and poses detected by an IMU device. The second method uses RFID tags to activate the predefined grasps so the user can interact with the environment. The third approach focuses on the use of computer vision and a dictionary-based platform to select the interactions of the prosthetic device. In sequence, the NASA Task Load Index procedure used to evaluate these interfaces is described in detail. In chapter 4, aspects of the results of the experiments are given: how the systems behave during the experiments with non-amputee and amputee and feedback from the users. Finally, this chapter concludes the dissertation.

# Bibliography

- ANDRADE, D. T. G.; PEREIRA, G. M.; NETO, A. R.; ROHMER, E. Human prosthetic interaction: Integration of several techniques. In: *SBAI 2017 - Simpósio Brasileiro de Automação Inteligente*. [S.l.: s.n.], 2017. p. 1209–1215. ISSN 2175 8905. Cited 2 times on pages 33 and 41
- Arduino Company. *Arduino Uno REV3*. 2017. <<https://store.arduino.cc/usa/arduino-uno-rev3>>. Accessed: 22/12/2017. Cited 2 times on pages 13 and 44
- BARNES, J.; DYSON, M.; NAZARPOUR, K. Comparison of hand and forearm muscle pairs in controlling of a novel myoelectric interface. In: IEEE. *Systems, Man, and Cybernetics (SMC), 2016 IEEE International Conference on*. [S.l.], 2016. p. 002846–002849. Cited on page 23
- BRITANNICA, T. E. of E. *Hand*. 2016. <<https://www.britannica.com/science/hand-anatomy>>. Accessed: 28/12/2017. Cited on page 18
- BUFFONE, B. *Touch Bionics i-limb prosthesis is controlled by an iPhone app*. 2013. <<https://www.cnet.com/news/touch-bionics-i-limb-prosthesis-is-controlled-by-an-iphone-app/>>. Accessed: 19/04/2018. Cited on page 15
- CONDORI, K. A.; URQUIZO, E. C.; DIAZ, D. A. Embedded brain machine interface based on motor imagery paradigm to control prosthetic hand. In: IEEE. *ANDESCON, 2016 IEEE*. [S.l.], 2016. p. 1–4. Cited on page 25
- CUTKOSKY, M. R.; HOWE, R. D. Human grasp choice and robotic grasp analysis. In: *Dextrous robot hands*. [S.l.]: Springer, 1990. p. 5–31. Cited 2 times on pages 18 and 19
- ENABLE. *Enabling the Future*. 2015. <<http://enablingthefuture.org/>>. (Accessed in 24/05/2017). Cited on page 15
- FAJARDO, J.; FERMAN, V.; LEMUS, A.; ROHMER, E. An affordable open-source multifunctional upper-limb prosthesis with intrinsic actuation. In: IEEE. *Advanced Robotics and its Social Impacts (ARSO), 2017 IEEE Workshop on*. [S.l.], 2017. p. 1–6. Cited on page 15
- FAJARDO, J.; LEMUS, A.; ROHMER, E. Galileo bionic hand: semg activated approaches for a multifunction upper-limb prosthetic. In: IEEE. *Central American and Panama Convention (CONCAPAN XXXV), 2015 IEEE Thirty Fifth*. [S.l.], 2015. p. 1–6. Cited on page 15
- GHAZAEI, G.; ALAMEER, A.; DEGENAAR, P.; MORGAN, G.; NAZARPOUR, K. Deep learning-based artificial vision for grasp classification in myoelectric hands. *Journal of Neural Engineering*, IOP Publishing, v. 14, n. 3, p. 036025, 2017. Cited on page 25

- GRIFFITHS, H. Treatment of the injured workman. *The Lancet*, Elsevier, v. 241, n. 6250, p. 729–733, 1943. Cited on page 18
- GUO, W.; SHENG, X.; LIU, H. *et al.* Mechanomyography assisted myoelectric sensing for upper-extremity prostheses: a hybrid approach. *IEEE Sensors Journal*, IEEE, 2017. Cited on page 24
- IBERALL, T. The nature of human prehension: Three dextrous hands in one. In: IEEE. *Robotics and Automation. Proceedings. 1987 IEEE International Conference on*. [S.l.], 1987. v. 4, p. 396–401. Cited on page 19
- KAPANDJI, A. Fisiologia articular: esquemas comentados de mecânica humana. são paulo: Panamericana. *Trad. Editorial Medica Panamericana SA*, Rio de Janeiro: Guanabara Koogan, 2000. Cited 6 times on pages 11, 20, 21, 22, 28, and 47
- KiCad EDA. *Ubuntu*. 20–. <<http://kicad-pcb.org/download/ubuntu/>>. Accessed: 05/01/2017. Cited on page 37
- KUMAR, D.; BASTOS, T.; ARJUNAN, S. *Devices for Mobility and Manipulation for People with Reduced Abilities*. [S.l.: s.n.], 2014. ISBN 9781466586451. Cited 3 times on pages 13, 22, and 23
- LANGEVIN, G. *inMoov Robot*. 201–. <<http://inmoov.fr/>>. (Accessed in 20/03/2017). Cited on page 27
- LYONS, D. A simple set of grasps for a dextrous hand. In: IEEE. *Robotics and Automation. Proceedings. 1985 IEEE International Conference on*. [S.l.], 1985. v. 2, p. 588–593. Cited 3 times on pages 11, 19, and 20
- MCBRIDE, E. D. *Disability evaluation*. Third edition. [S.l.]: Philadelphia, London, Montreal: J. B. Lippincott Company, 1942. Cited 2 times on pages 18 and 19
- MCMULLEN, D. P.; HOTSON, G.; KATYAL, K. D.; WESTER, B. A.; FIFER, M. S.; MCGEE, T. G.; HARRIS, A.; JOHANNES, M. S.; VOGELSTEIN, R. J.; RAVITZ, A. D. *et al.* Demonstration of a semi-autonomous hybrid brain–machine interface using human intracranial eeg, eye tracking, and computer vision to control a robotic upper limb prosthetic. *IEEE Transactions on Neural Systems and Rehabilitation Engineering*, IEEE, v. 22, n. 4, p. 784–796, 2014. Cited on page 25
- MSC, P. E. S.; PHD, P. K. E. Electromyogram pattern recognition for control of powered upper-limb prostheses: State of the art and challenges for clinical use. *Journal of rehabilitation research and development*, Superintendent of Documents, v. 48, n. 6, p. 643, 2011. Cited on page 23
- MURGUIALDAY, A. R.; AGGARWAL, V.; CHATTERJEE, A.; CHO, Y.; RASMUSSEN, R.; O'ROURKE, B.; ACHARYA, S.; THAKOR, N. V. Brain-computer interface for a prosthetic hand using local machine control and haptic feedback. In: IEEE. *Rehabilitation Robotics, 2007. ICORR 2007. IEEE 10th International Conference on*. [S.l.], 2007. p. 609–613. Cited 2 times on pages 23 and 24

- NAPIER, J. R. The prehensile movements of the human hand. *Bone & Joint Journal*, Bone and Joint Journal, v. 38, n. 4, p. 902–913, 1956. Cited on page 19
- NASA. *NASA-TLX*. 2011. <<http://www.nasatlx.com/>>. (Accessed in 20/03/2017). Cited 3 times on pages 54, 56, and 57
- NXP SEMICONDUCTORS. *Standard performance MIFARE and NTAG frontend*. [S.l.], 2016. Rev. 3.9. Cited 2 times on pages 13 and 43
- OPPUS, C. M.; PRADO, J. R. R.; ESCOBAR, J. C.; MARIÑAS, J. A. G.; REYES, R. S. Brain-computer interface and voice-controlled 3d printed prosthetic hand. In: IEEE. *Region 10 Conference (TENCON), 2016 IEEE*. [S.l.], 2016. p. 2689–2693. Cited on page 24
- Orthoworx Orthotics and Prosthetics. *Body-powered Arm Prosthesis*. 201–. <<http://www.orthoworx.co.za/prosthetics/upper-extremity-prosthetics/body-powered-arm-prosthesis/>>. Accessed: 02/01/2018. Cited on page 22
- Ottobock US. *Body-powered prosthetic solutions*. 201–. <<https://www.ottobockus.com/prosthetics/upper-limb-prosthetics/solution-overview/body-powered-prosthetic-solutions/>>. Accessed: 02/01/2018. Cited on page 22
- Raspberry Pi Foundation. *Camera Module*. 201–. <<https://www.raspberrypi.org/documentation/hardware/camera/README.md>>. Accessed: 22/12/2017. Cited on page 49
- RHEE, T.; NEUMANN, U.; LEWIS, J. P. Human hand modeling from surface anatomy. In: ACM. *Proceedings of the 2006 symposium on Interactive 3D graphics and games*. [S.l.], 2006. p. 27–34. Cited on page 18
- ROHMER, E.; SINGH, S. P.; FREESE, M. V-rep: A versatile and scalable robot simulation framework. In: IEEE. *Intelligent Robots and Systems (IROS), 2013 IEEE/RSJ International Conference on*. [S.l.], 2013. p. 1321–1326. Cited on page 27
- SCHLESINGER, G. *Ersatzglieder und Arbeitshilfen: Für Kriegsbeschädigte und Unfallverletzte*. [S.l.]: Springer Berlin Heidelberg, 1919. 321–661 p. Cited 3 times on pages 11, 18, and 19
- SCHWARZ, R. J.; TAYLOR, C. L. The anatomy and mechanics of the human hand. *Artificial limbs*, v. 22, 1955. Cited on page 18
- SLEVINSKY, M. *GUI without the G: Going Beyond the Screen with the Myo<sup>TM</sup> Armband*. 2014. <<http://developerblog.myo.com/gui-without-g-going-beyond-screen-miotm-armband/>>. Accessed: 20/03/2017. Cited 2 times on pages 11 and 34
- SLOCUM, D. B.; PRATT, D. R. Disability evaluation for the hand. *JBJS*, LWW, v. 28, n. 3, p. 491–495, 1946. Cited 2 times on pages 18 and 19
- STANDING, S. Grays anatomia a base anatómica da prática clínica. *Trad. Denise Costa Rodrigues et al*, v. 4, 2010. Cited 2 times on pages 18 and 30

Thalmic Labs Inc. *About the Myo Armband*. 2016. <<https://jp.myo.com/education>>. Accessed: 05/01/2018. Cited 2 times on pages 11 and 30

Thalmic Labs Inc. *Myo*. 2016. <<https://www.myo.com/techspecs>>. Accessed: 30/03/2018. Cited 2 times on pages 29 and 30

Touch Bionics Inc. *i-limb Mobile Apps*. 2018. <<http://www.touchbionics.com/products/i-limb-mobile-apps>>. (Accessed in 20/01/2018). Cited on page 15

TRACHTENBERG, M. S.; SINGHAL, G.; KALIKI, R.; SMITH, R. J.; THAKOR, N. V. Radio frequency identification—an innovative solution to guide dexterous prosthetic hands. In: IEEE. *Engineering in Medicine and Biology Society, EMBC, 2011 annual international conference of the IEEE*. [S.l.], 2011. p. 3511–3514. Cited 2 times on pages 24 and 26

TUBIANA, R.; THOMINE, J.-M.; MACKIN, E. Diagnóstico clínico da mão e do punho. In: *Diagnóstico clínico da mão e do punho*. [S.l.: s.n.], 1996. Cited on page 18

ZHU, D. *myo-raw*. [S.l.]: GitHub, 2014. <<https://github.com/dzhu/myo-raw>>. Cited 2 times on pages 30 and 31

# Appendix

## APPENDIX A – Ethical Committe Approval



## **TERMO DE CONSENTIMENTO LIVRE E ESCLARECIDO – Linha de pesquisa IV (Anexo VI)**

**Projeto XTReMe: Experiências de Tecnologias para Reabilitação em Medicina**

**Subprojeto: Estudo e desenvolvimento de próteses de mão robóticas**

**Pesquisadores responsáveis: Eric Rohmer**

**CAAE: 58592916.9.1001.5404**

Você está sendo convidado a participar como voluntário da pesquisa “Estudo e desenvolvimento de próteses de mão robóticas”. Este documento, chamado Termo de Consentimento Livre e Esclarecido, visa assegurar seus direitos como participante e é elaborado em duas vias, uma que deverá ficar com você e outra com o pesquisador.

Por favor, leia com atenção e calma, aproveitando para esclarecer suas dúvidas. Se houver perguntas antes ou mesmo depois de assiná-lo, você poderá esclarecê-las com o pesquisador. Se preferir, pode levar este Termo para casa e consultar seus familiares ou outras pessoas antes de decidir participar. Não haverá nenhum tipo de penalização ou prejuízo se você não aceitar participar ou retirar sua autorização em qualquer momento.

### **Justificativa e objetivos:**

Próteses e órteses inteligentes de mão de alta tecnologia oferecem a possibilidade de escolher vários tipos de ações para os dedos, indo além do simples abrir e fechar de mão. Por exemplo, algumas próteses importadas oferecem dezenas de ações possíveis como apontar para digitar, segurar objetos pequenos com dois dedos ou até a pegada para utilizar um mouse. Porém, possuem um custo extremamente alto, chegando a milhares de dólares ou podem ainda nem estar disponíveis para o mercado. De fato, deixando o acesso à essa tecnologia indisponível a centenas de brasileiros.

Adicionalmente, com as próteses inteligentes importadas, a seleção da ação desejada pelo usuário é realizada por muitas contrações musculares diferentes e conseguir a escolha certa necessita de um treinamento cotidiano intensivo e muito fatigante com a prótese para um resultado que pode ser frustrante.

Visando reverter esse cenário, procura-se oferecer um produto brasileiro, de fácil manutenção, personalizado e semelhante em funcionalidades, mas com uma seleção de movimentos mais robusta e intuitiva por um preço muito mais acessível (usando a tecnologia de impressão 3D e componente de prateleiras).

Sendo assim, o objetivo desta pesquisa é testar os protótipos com o público alvo e refinar as técnicas de seleções das ações, bem como a confiabilidade e conforto de uso da prótese.

Neste documento, prótese se refere tanto a próteses quanto a órteses inteligentes (i.e. que tem interações que se adaptam às necessidades do usuário). Além disso, interfaces (homem-máquina) são definidas como um conjunto de sensores e as interações do usuário com os estes sensores.

As interfaces que selecionam as ações dos dedos consideradas nesta pesquisa são baseadas no uso combinado de eletromiografia (EMG) para avisar a prótese do começo do processo de seleção da ação. Em seguida, seleciona-se a ação por comando de voz, aplicação de celular, movimento, chips fixos em objetos ou outros. Finalmente, o EMG define o momento de realização da ação.

### **Procedimentos:**

Rubrica do pesquisador: \_\_\_\_\_ Rubrica do participante: \_\_\_\_\_

Participando do estudo você está sendo convidado a utilizar uma interface para o controle da prótese de mão no simulador através de uma ou várias interfaces de interação, tais como comandos por voz, sensores de gestos e eletromiografia. Além disso, você também poderá ser convidado a utilizar uma prótese robótica de mão real e realizar as mesmas interações descritas anteriormente.

Em ambos os casos apresentados, um terceiro estará sempre acompanhando o procedimento podendo, eventualmente, pará-lo, se necessário. Você poderá ser convidado mais de uma vez para realizar os testes a fim de analisarmos a sua evolução no uso das interfaces e sua opinião sobre a usabilidade e ergonomia com relação a todas as interfaces apresentadas.

O local de realização dos testes será dentro do Laboratório de Computação e Automação da Faculdade de Engenharia Elétrica e Computação da UNICAMP. O tempo total estimado para realização dos testes não deve ser superior a 2 (duas) horas. Caso os resultados forem conclusivos e caso você tenha interesse e se sinta confortável poderemos pedir para que a prótese seja utilizada por você durante uma semana durante o seu cotidiano. Ao final da semana, você dará retorno sobre a sua experiência de uso.

Os procedimentos que serão realizados são descritos detalhadamente a seguir:

1. Demonstração: chegando ao local do teste, você será apresentado à prótese de mão (virtual ou real) e os sensores a serem utilizados. Os detalhes da prótese serão mostrados e o pesquisador responsável irá explicar como ela pode ser manipulada através das demonstrações. O tempo estimado para essa etapa é de 10 a 20 minutos, dependendo do número de interfaces que irão ser demonstradas.
2. Posicionamento da prótese no usuário: nesta etapa, o membro da equipe que fez a demonstração irá retirar os sensores que estava utilizando para fazer a demonstração e irá colocá-los em você. Se a prótese real estiver disponível, esta será usada ao invés da prótese virtual. Você será perguntado se se sente confortável ao utilizar o sistema e, caso não esteja, pode retirar a qualquer momento. Tempo estimado para essa etapa é de 5 a 10 minutos.
3. Uso da prótese via interface homem-máquina: você poderá ser convidado a: a) Utilizar uma interface para controlar a prótese (até 60 minutos de duração); b) Utilizar mais uma interface para controlar a prótese ou repetir o teste anterior com a mesma interface (até 30 minutos de duração); c) Caso esteja testando com a prótese real, apenas colocar a prótese para descrever se peso, tamanho e outras características do produto estão adequadas e sua opinião sobre a estética do mesmo (até 30 minutos de duração); O tipo de interface utilizada será definido pela equipe. Entretanto, você poderá desistir a qualquer momento do teste se, eventualmente, não se sentir confortável com as decisões da equipe.
4. Calibração: neste teste você estará com a prótese e tentará se familiarizar com os tipos de comandos que devem ser enviados a prótese. Você tentará repetir as interações demonstrados pela equipe para que o sistema se adeque à sua forma de interação.
5. Práticas com a interface: nesta etapa você tentará controlar os diferentes tipos de ações que são possíveis através do sistema. Você, por exemplo, tentará manusear um mouse, pegar uma caneta, pegar uma bola, tomar um copo com água, segurar

Rubrica do pesquisador: \_\_\_\_\_ Rubrica do participante: \_\_\_\_\_

uma maleta (leve e sem objetos dentro), apontar para algum objeto, fechar as mãos, segurar uma serrinha de unha, utilizar um borrifador de água, manusear talheres, abrir a mão, relaxar a mão, entre outros eventos do cotidiano.

6. Entrevista: você é a parte essencial no desenvolvimento desse projeto. Dessa forma, queremos saber a sua opinião sobre a sua experiência em utilizar a prótese de mão. Será realizada uma entrevista com áudio e vídeo onde será perguntado o que você achou da sua experiência, quais suas sugestões, quais as suas críticas e quais as suas expectativas. A entrevista será realizada durante o treinamento do uso da prótese.

**Desconfortos e riscos:**

Os riscos possíveis relacionados aos procedimentos descritos acima incluem desconforto muscular durante o uso da prótese.

**Benefícios:**

A sua participação nesta pesquisa não implicará em nenhum benefício pessoal e não é obrigatória.

**Acompanhamento e assistência:**

Caso queira, você poderá desistir da sua participação a qualquer momento, sem que isso lhe cause nenhum prejuízo. Você será acompanhado e assistido pelo pesquisador responsável e a sua equipe durante esses procedimentos, podendo fazer perguntas sobre qualquer dúvida que apareça durante todo o estudo.

**Sigilo e privacidade:**

Os dados coletados estarão sob o resguardo científico e o sigilo profissional, e contribuirão para o alcance dos objetivos deste trabalho e para posteriores publicações dos dados.

**Ressarcimento e indenização:**

Você não receberá nenhum pagamento por sua participação nesta pesquisa, mas caso venha a ter despesas de transporte ou alimentação para participar na pesquisa, será ressarcido.

**Métodos alternativos:**

Não há métodos alternativos.

**Contato:**

Para quaisquer dúvidas, você pode contatar os pesquisadores responsáveis: Dr. Eric Rohmer (tel. (19)352-10247, email: [eric@dca.fee.unicamp.br](mailto:eric@dca.fee.unicamp.br), endereço: Faculdade de Engenharia Elétrica e Computação - Av. Albert Einstein, 400, UNICAMP, CEP: 13083-859, Cidade Universitária, Campinas, SP).

Em caso de denúncias ou reclamações sobre sua participação e sobre questões éticas do estudo, você poderá entrar em contato com a secretaria do Comitê de Ética em Pesquisa (CEP) da UNICAMP das 08:30hs às 11:30hs e das 13:00hs às 17:00hs na Rua: Tessália Vieira de Camargo, 126; CEP 13083-887 Campinas – SP; telefone (19) 3521-8936 ou (19) 3521-7187; e-mail: [cep@fcm.unicamp.br](mailto:cep@fcm.unicamp.br).

Rubrica do pesquisador: \_\_\_\_\_ Rubrica do participante: \_\_\_\_\_

**O Comitê de Ética em Pesquisa (CEP).**

O papel do CEP é avaliar e acompanhar os aspectos éticos de todas as pesquisas envolvendo seres humanos. A Comissão Nacional de Ética em Pesquisa (CONEP), tem por objetivo desenvolver a regulamentação sobre proteção dos seres humanos envolvidos nas pesquisas. Desempenha um papel coordenador da rede de Comitês de Ética em Pesquisa (CEPs) das instituições, além de assumir a função de órgão consultor na área de ética em pesquisas

**Consentimento livre e esclarecido:**

Após ter recebido esclarecimentos sobre a natureza da pesquisa, seus objetivos, métodos, benefícios previstos, potenciais riscos e o incômodo que esta possa acarretar, aceito participar e declaro estar recebendo uma via original deste documento assinada pelo pesquisador e por mim, tendo todas as folhas por nós rubricadas:

Nome do (a) participante: \_\_\_\_\_

Contato telefônico: \_\_\_\_\_

e-mail (opcional): \_\_\_\_\_

\_\_\_\_\_, Data: \_\_\_\_/\_\_\_\_/\_\_\_\_.  
(Assinatura do participante ou nome e assinatura do seu RESPONSÁVEL LEGAL)

**Responsabilidade do Pesquisador:**

Asseguro ter cumprido as exigências da resolução 466/2012 CNS/MS e complementares na elaboração do protocolo e na obtenção deste Termo de Consentimento Livre e Esclarecido. Asseguro, também, ter explicado e fornecido uma via deste documento ao participante. Informo que o estudo foi aprovado pelo CEP perante o qual o projeto foi apresentado. Comprometo-me a utilizar o material e os dados obtidos nesta pesquisa exclusivamente para as finalidades previstas neste documento ou conforme o consentimento dado pelo participante.

\_\_\_\_\_, Data: \_\_\_\_/\_\_\_\_/\_\_\_\_.  
(Assinatura do pesquisador)

Rubrica do pesquisador: \_\_\_\_\_ Rubrica do participante: \_\_\_\_\_

## APPENDIX B – Identification Form

## Identification form

Volunteer ID: \_\_\_\_\_

Age: \_\_\_\_\_

Gender: ( ) Female ( ) Male

Level of education

( ) Elementary school

( ) High school

( ) Bachelor or equivalent

( ) Post-doctoral or equivalent

Volunteer has any level of amputation? ( ) Yes ( ) No

If the volunteer is an amputee:

What is your level of amputation?

( ) Shoulder disarticulation

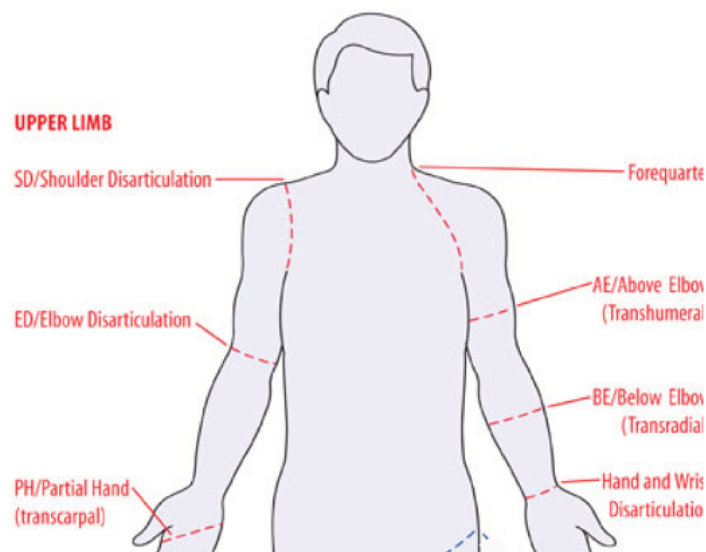
( ) Wrist disarticulation

( ) Transhumeral

( ) Transcarpal

( ) Elbow disarticulation

( ) Transradial



What is the approximate size of the residual segment/limb? \_\_\_\_\_

For how long you are an amputee? \_\_\_\_\_

What was the amputated side? \_\_\_\_\_

Was your amputated side the dominant one? ( ) Yes ( ) No

Have you ever used a prosthesis? ( ) Yes ( ) No

If so, which one? \_\_\_\_\_

If you already used a prosthesis, for how long you have been using it? \_\_\_\_\_

## APPENDIX C – Questionnaire

1. Describe your experience. What did you find it was hard to do?
2. In your opinion, can this technology be used in real prosthesis?
3. Do you have suggestions that help us to improve the system?

## APPENDIX D – Source code

<https://gitlab.com/dandara/prosthesis.git>



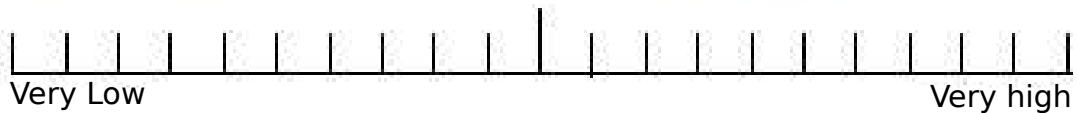
## Annex

# ANNEX A – NASA Task Load Index: Rating sheet

ID	Task	Date
----	------	------

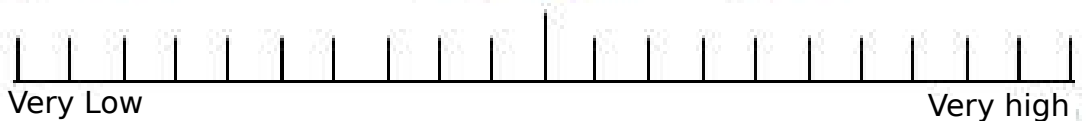
**Mental Demand**

How much mental and perceptual activity was required?  
Was the task easy, simple or complex and exacting?



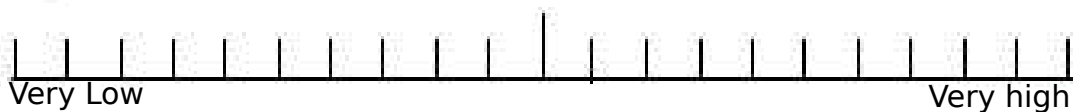
**Physical Demand**

How much physical activity was required?  
Was the task easy or demanding? Restful or Laborious?



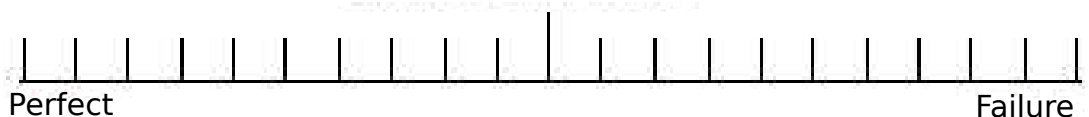
**Temporal Demand**

How hurried or rushed was the pace of the task?



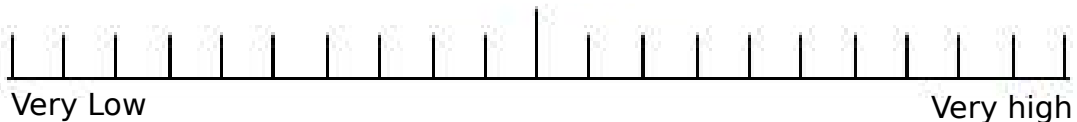
**Performance**

How successful were you in accomplishing  
what you were asked to do?



**Effort**

How hard did you have to work to accomplish  
your level of performance?



**Frustration Level**

How insecure, discouraged, irritated, stressed,  
and annoyed were you?

